

UNCLASSIFIED

SECURITY CLASSIFICATION OF THIS PAGE (When Data Entered)

REPORT DOCUMENTATION PAGE

READ INSTRUCTIONS
BEFORE COMPLETING FORM

1. REPORT NUMBER AFIT/GEOPH/78-2	2. GOVT. ACCESSION NO.	3. RECIPIENT'S CATALOG NUMBER
4. TITLE (and Subtitle) HIGH POWER CONTINUOUS WAVE SEMICONDUCTOR INJECTION LASER	5. TYPE OF REPORT & PERIOD COVERED M.S. Thesis	
6. AUTHOR(s) John C. Griffin, III	7. CONTRACT NUMBER	
8. PERFORMING ORGANIZATION NAME AND ADDRESS Air Force Institute of Technology (AFIT-EN) Wright-Patterson AFB, Ohio 45433	9. PROGRAM ELEMENT, PROJECT, TASK AREA & REPORT NUMBER	
10. CONTROLLING OFFICE NAME AND ADDRESS Air Force Avionics Laboratory Wright-Patterson AFB OH 45433	11. REPORT DATE December 1978	12. NUMBER OF PAGES 76
13. MONITORING AGENCY NAME & ADDRESS (if different from Controlling Office)	14. SECURITY CLASS. (of this report) Unclassified	
15a. DECLASSIFICATION/DOWNGRADING SCHEDULE		

16. DISTRIBUTION STATEMENT (of this Report)

Approved for public release; distribution unlimited.

DDC

17. DISTRIBUTION STATEMENT (of the abstract entered in Block 20, if different from Report)

FEB 22 1979

18. SUPPLEMENTARY NOTES

Approved for public release AFR190-17
 Joseph P. Hippe, Major, USAF
 Director of Information 19 Jan 79

19. KEY WORDS (Continue on reverse side if necessary and identify by block number)

Gallium Arsenide
 High Power Semiconductor Laser
 Injection Laser
 Semiconductor Laser

20. ABSTRACT (Continue on reverse side if necessary and identify by block number)

A review of fundamental semiconductor laser theory is presented, followed by a theoretical analysis of the figures of merit, which affect high power CW operation. It is postulated that high CW power of the order of several watts can be obtained from long lasers with low end reflectivities. The removal of heat from the junction region can be best accomplished in narrow lasers with a width near 50 micrometers. Further optimization

ADA064758

DDC FILE COPY

UNCLASSIFIED

SECURITY CLASSIFICATION OF THIS PAGE (When Data Entered)

of output power can be achieved in devices with a thin optical cavity. However, the optical cavity must be sufficiently thick to provide an output facet area large enough to accommodate high optical flux, without experiencing catastrophic damage. Diffused homojunction structures are not suitable for implementing these parameters. A Large Optical Cavity, epitaxially grown heterostructure device appears to be the most suitable structure for high power CW operation. Trends in output power with varying laser length, width, reflectivity, and cavity thickness are presented graphically.

HIGH POWER CONTINUOUS WAVE
SEMICONDUCTOR INJECTION LASER

THESIS

AFIT/GEO/PH/78-2 John C. Griffin, III
Capt USAF

Approved for public release; distribution unlimited.

79 01 30

HIGH POWER CONTINUOUS WAVE
SEMICONDUCTOR INJECTION LASER

THESIS

Presented to the Faculty of the School of Engineering
of the Air Force Institute of Technology

Air Training Command
in Partial Fulfillment of the
Requirements for the Degree of
Master of Science

by

John C. Griffin, III, B.S.

Capt USAF

Graduate Electro-Optics

December 1978

ADMINISTRATIVE	
DATE	DATE RECEIVED <input checked="" type="checkbox"/>
NO.	DATE RECEIVED <input checked="" type="checkbox"/>
APPROVED	<input checked="" type="checkbox"/>
JUSTIFICATION	
BY	
SUGGESTION/AVAILABILITY CODE	
DATE	DATE RECEIVED <input checked="" type="checkbox"/>
A	

Approved for public release; distribution unlimited.

01 30 34

Preface

At the time of the writing of this thesis, there has been very little work accomplished in the area of high power Continuous Wave (CW) semiconductor lasers. The current emphasis in the development of semiconductor laser technology is centered about low power applications in the area of optical communications and integration of the lasers with fiber optics. The principal interest in high power CW devices is for use as illuminators and range finders in reconnaissance systems developed for military applications. Consequently, there does not exist, to my knowledge, any publication which treats the recent technological developments, in the field of semiconductor lasers, in the perspective of high power applications. In my treatment of this problem, I have divided the thesis into two parts. In the first part, consisting of Chapters I, II, and III, I will present the basic information that is known today about semiconductor lasers. In the second part, consisting of Chapters IV, V, and VI, I will apply this information to the special case of the high power CW laser, to determine what parameters can be optimized to achieve the maximum CW output power from the device.

The plots of output power as a function of length, width and reflectivity in Chapters IV and V are intended to show the trends in P_{out} as the different parameters are

varied. Although these trends are quite spectacular, particularly with respect to changing length, the numerical values of P_{out} indicated should be interpreted with caution. The output power of a real device will approach these values, depending on the purity of the semiconductor material and the uniformity of the optical cavity formed by the crystal growth process.

Thanks are due to Dr. Ron Paulson and Dr. Brad Sowers of the Electro-Optics branch of the Air Force Avionics Laboratory, who have provided me with the practical motivation to pursue this topic. Thanks are also due to Dr. Bob Henghold of the AFIT Physics Department for his support. I wish to especially thank my thesis advisor, Dr. Ted Luke of the AFIT Physics Department for his continued and extremely valuable assistance and encouragement during my pursuit of the solution to this problem. I believe a very special acknowledgement is appropriate for the continued support of my wonderful family--wife Janet, son John, and my late mother Sally, who passed away in March. I wish to express a final note of thanks to my typist, Mrs. Olivia Davis.

John C. Griffin, III

Contents

	Page
Preface	ii
List of Figures	v
Notation	vii
Abstract	x
I. Introduction	1
Background	1
Statement of the Problem	4
Assumptions	4
Approach	5
II. Fundamental Semiconductor Laser Theory	7
Fundamental Laser Theory	7
Emission and Absorption of Radiation in the Semiconductor	11
Output Power of the Semiconductor Laser	16
III. The Semiconductor Laser	18
The Homojunction Laser	18
The Heterojunction Laser	18
The Optical Cavity	23
IV. Optimization of the Laser Design for Maximum Output Power	27
The Material	27
The Cavity	28
Optimization of the Cavity Dimensions	28
Internal Absorption and Diffraction Effects	36
The Laser Structure	40
Stripe Geometry	42
Summary	43
V. Thermal Effects	45
VI. Conclusions and Recommendations	52
Bibliography	55
Appendix: Laser Degradation	61
Vita	65

List of Figures

<u>Figure</u>	<u>Page</u>
1 Modulation imposed on CW semiconductor laser .	3
2 Energy Band Diagram of Degenerate p-n Junction (a) $V = 0$; (b) $V = E_g/e$	13
3 Energy Band Diagram of (a) Direct Bandgap Material and (b) Indirect Bandgap Material . .	14
4 Mode Volume (Product dLW) encompassing the optical mode emitted from a p-n junction with Carrier Recombination Region consisting of volume product tLW	15
5 Typical Homojunction Laser	19
6 Large Optical Cavity Heterostructure Laser proposed by Lockwood et al.	20
7 Typical Heterostructure Lasers with a qualita- tive representation of bandgap, E_g , and index of refraction, n . (a) SH Laser; (b) DH Laser; (c) TH Laser; (d) QH Laser	22
8 Optical Cavities Other Than Fabry-Perot: (a) Circular, (b) Triangular, (c) Rectangular (Four sides polished)	24
9 Typical Fabry-Perot Cavity	26
10 Typical Distributed Feedback Laser	26
11 Typical Ring Laser	26
12 Output Power vs Cavity Length for Different Values of Cavity Width	30
13 Output Power vs Length and Reflectivity for Different Values of Width	32
14 Output Power vs Cavity Thickness	35
15 Theoretical and Experimental Absorption Due to Diffraction vs Laser Length	38
16 Output Power vs Laser Length for Different Values of Width With Values of α from Fig. 15 .	39

17	Typical oxide insulated Stripe Geometry Heterostructure Laser	43
18	Thermal Heat Flow Model for oxide insulated stripe geometry heterostructure laser proposed by Garel-Jones	44
19	Double-Sided heat sink proposed by Marinace . .	46
20	Stimulated Power vs Laser Length for Different Values of Width	50

Notation

A	Cross sectional area of laser diode equal to product LW.
A_{21}	Einstein "A" coefficient defined as the probability per unit time of spontaneous emission resulting from a state 2 to state 1 atomic transition.
B_{21}	Einstein "B" coefficient defined as the probability per unit time of stimulated emission from state 2 to state 1 atomic transition resulting from exposure to radiation.
B_{12}	Einstein "B" coefficient defined as the probability per unit time of a state 1 to state 2 atomic transition resulting from absorption of radiation.
C	Parameter defined as $(1/L)\ln(1/R)$.
c	Velocity of light in free space (3.0×10^8 m/sec).
d	Thickness of an optical cavity.
E	Energy.
E_f	Fermi Level.
E_{fc}	Conduction Band Fermi Level.
E_{fv}	Valence Band Fermi Level.
E_g	Energy Bandgap.
e	Electronic charge (1.602×10^{-19} Coul).
e	Exponential (2.718).
C	Constant that depends on the scattering losses at the sidewall of the Fabry-Perot cavity.
$g(\nu)$	Lineshape function.
h	Planck's constant (6.626×10^{-34} Joule-sec).
I	Current.
I_t	Threshold current.
I_ν	Intensity of radiation.
J	Current density.

J_t	Threshold current density.
$K(k)$	Complete elliptic integral of the first kind.
k	Boltzmann's constant (1.38×10^{-23} Joule/deg K).
L	Length of the optical cavity.
\ln	Natural logarithm.
N_1	Number of atoms per unit volume in state 1.
N_2	Number of atoms per unit volume in state 2.
n	Index of refraction.
n_1	Number of electrons in state 1.
n_2	Number of electrons in state 2.
P	Power.
P_{out}	Output power of laser.
P_{stim}	Power due to stimulated emission.
q	Integer (1,2,3,4.....).
R	Square root of the product of laser facet reflectivities $(r_1 r_2)^{1/2}$.
R_s	Series resistance.
r_1	Reflectivity of laser facet 1.
r_2	Reflectivity of laser facet 2.
t	Thickness of active region (carrier recombination region).
t_{spon}	Lifetime of a spontaneous transition.
t_{recom}	Time required for an electron hole recombination.
T	Temperature.
V	Voltage.
W_{12}	Transition rate from atomic state 1 to atomic state 2.
W_{21}	Transition rate from atomic state 2 to atomic state 1.

$W_i(\nu)$	Induced transition rate.
Z_{th}	Spreading resistance.
z	Longitudinal distance into lasing medium.
α	Total internal absorption coefficient.
α_D	Absorption coefficient due to diffraction.
α_{fc}	Absorption coefficient due to free carrier absorption.
α_s	Absorption coefficient due to scattering.
$\beta(\nu)$	Laser gain factor.
γ	Temperature dependent laser performance factor.
η_i	Internal quantum efficiency.
η_{ext}	External quantum efficiency.
κ	Thermal conductivity.
λ	Wavelength of radiation in free space.
ν	Frequency of radiation.
ρ	Electrical resistivity.
$\rho(\nu)$	Energy density.

Abstract

A review of fundamental semiconductor laser theory is presented, followed by a theoretical analysis of the figures of merit, which affect high power CW operation. It is postulated that high CW power of the order of several watts can be obtained from long lasers with low end reflectivities. The removal of heat from the junction region can be best accomplished in narrow lasers with a width near 50 micrometers. Further optimization of output power can be achieved in devices with a thin optical cavity. However, the optical cavity must be sufficiently thick to provide an output facet area large enough to accommodate high optical flux, without experiencing catastrophic damage. Diffused homojunction structures are not suitable for implementing these parameters. A Large Optical Cavity, epitaxially grown heterostructure device appears to be the most suitable structure for high power CW operation. Trends in output power with varying laser length, width, reflectivity, and cavity thickness are presented graphically.

HIGH POWER CONTINUOUS WAVE SEMICONDUCTOR INJECTION LASER

I. Introduction

Background

The ability to conduct real time battlefield surveillance during an armed conflict has become increasingly important to our military commanders in recent years. Conventional methods of reconnaissance (such as photography) require far too much time between the moment when the army field commander submits his request for reconnaissance and the time when he receives his information. Moderate success has been achieved in recent years through the use of systems such as the UPD-4 Side Looking Radar System (SLR), manufactured by Goodyear Aerospace Corporation. This system is currently deployed in Europe aboard the RF-4C aircraft and has data-link capability, which has provided military commanders with real time information about major battlefield movements during the simulated combat Reforger exercises in Germany each fall, since 1976. There are, however, limitations on the resolution of this system.

Recent advances in Electro-Optical technology have generated interest in the feasibility of an electro-optical real time imagery gathering system for tactical reconnaissance applications. The KA-98/Day-Night Sensor system

manufactured by the Perkin-Elmer Corporation was recently tested in a Remotely Piloted Vehicle (RPV) (Ref 1) and is also suitable for use in a manned aircraft such as the RF-4C. This system utilizes a liquid nitrogen cooled Gallium Arsenide semiconductor laser to provide illumination in conjunction with a silicon detector.

Planned development of systems similar to, but more sophisticated than the KA-98 has indicated the need for an illumination source capable of high power output and rapid frequency response (Ref 2). The frequency at which GaAs lasers can be successfully modulated, via pulsed modulation of the input current is ultimately limited by the drift velocity of the electrons in the material (Ref 3:284). Semiconductor lasers can be modulated at high frequencies (in the GHz range) if they are operated Continuous Wave (CW) and the modulation is imposed on the CW output as shown in Fig. 1. This technique has been used quite successfully for the low power CW case, in the area of high bit rate fiber optical communications systems (Ref 4;5). However, very little work has been done for the high power (greater than 1 Watt) CW case. Ternary heterostructure GaAs-AlGaAs lasers capable of CW output as high as 2.5 Watts were fabricated by Laser Diode Laboratories in 1976 under contract with the Air Force Avionics Laboratory (Ref 6:50). These devices were tested at the Air Force Institute of Technology (as part of a master's degree thesis in 1977) under CW and RF current modulated (25 MHz) conditions

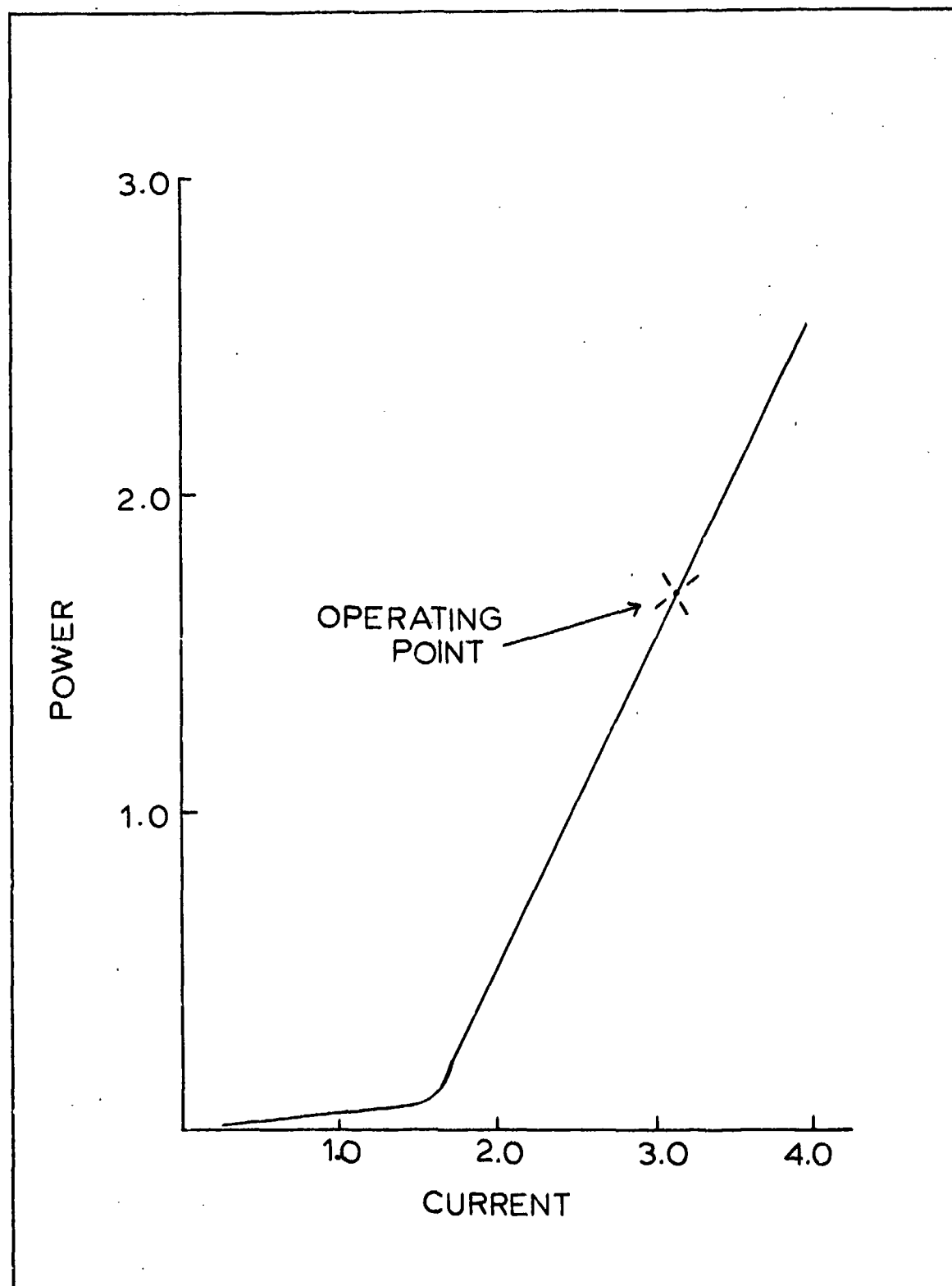


Fig. 1. Modulation imposed on CW semiconductor laser (units of current and power arbitrary) (Adapted from Ref 4:305)

(Ref 7:41). Although the devices were successfully operated CW, catastrophic failure of three devices, which were RF modulated, occurred (Ref 7:41). The requirement for further study of the operating parameters affecting the CW output of a semiconductor laser formed the motivation for the present thesis.

Statement of the Problem

The broad problem is to determine the best possible combination of semiconductor material and laser structure that will result in a device which will yield a high power (greater than 1 Watt) CW output; and can be successfully RF modulated. The first step in the solution of this broad problem comprises the specific problem to be addressed in this thesis: namely, what are the optimum material parameters and the optimum laser structure, which will provide a device capable of maximum CW output power.

Assumptions

For the purpose of this thesis, Gallium Arsenide has been selected as the basic laser material. The motivation behind this assumption was to reduce the number of variables in the overall problem of optimizing output power, by starting with a material about which a substantial amount of information was currently available. GaAs has been the most popular choice for development and was chosen for the purposes of this thesis, since it is a direct-bandgap semiconductor, and has comparatively good thermal conductivity

at low temperatures. The advantages of these characteristics will be discussed in Chapter IV.

Approach

The thesis will consist of two sections. In the first section, the basic figures of merit of a semiconductor laser will be studied to determine their relationship to each other and ultimately to the output power of the laser. In the second, the various structures of the GaAs laser will be studied to determine how the figures of merit for high power operation might be realized.

In Chapter II, paralleling a treatment by Yariv, the fundamental theory governing the operation of all lasers will be presented. This theory will then be applied to the special case of the semiconductor laser, leading to general expressions for the threshold current and output power of these devices. The existing homojunction and heterojunction lasers as well as the different types of optical cavities will be presented in Chapter III.

In Chapter IV, a Gallium Arsenide device operating in a Fabry-Perot cavity is assumed. The effect of changing laser length, reflectivity, width, optical cavity thickness, and carrier recombination region thickness on the output power is presented graphically. It will be shown that long lasers with low end reflectivities are theoretically capable of producing high CW output power of the order of several watts. Output power can be further optimized in

devices with thin optical cavities. However, the optical cavity must be sufficiently thick to provide an output facet area large enough to withstand high optical flux without experiencing catastrophic failure. The Large Optical Cavity heterostructure laser appears to be the most suitable structure for implementing these results, due to the fact that a thin carrier recombination region (less than 1 micrometer) can be maintained within a relatively thick optical cavity several micrometers thick.

Thermal effects resulting from junction heating will be discussed in Chapter V. It will be shown that increasing laser length while maintaining a relatively small width will result in increased output power, without significantly increasing the junction operating temperature.

Finally, a discussion of the various laser degradation phenomena, including catastrophic laser degradation, will be presented in the Appendix.

II. Fundamental Semiconductor Laser Theory

The basic relationships describing the generation of coherent radiation will be developed in the first part of this section. These relationships are valid for all types of lasers. Next, the properties of semiconductors will be discussed and the basic laser relationships will be applied to the special case of the semiconductor. An expression for the threshold current for lasing in a semiconductor laser will be obtained. Finally, an expression for the total output power of the semiconductor laser will be presented.

Fundamental Laser Theory

The operation of any laser is characterized by the stimulated emission of radiation. This stimulated emission is one of three dominant processes that occur in an atomic system subjected to electromagnetic radiation; the other two are absorption and spontaneous emission. It is important to establish the relationship between the intensity, I , of the radiation incident on the lasing medium, and the transition rates for the three processes mentioned above. The following derivation follows the treatment of this problem by Yariv (Ref 8:94-98).

The assumption will be made that there now exists a collection of identical atoms, capable of two distinct

energy states, subjected to a radiative field of energy density distributed in frequency uniformly about the transition frequency. This energy density is defined as $\rho(\nu)$. The transition rate per atom from state 2 to 1 is defined as W_{21} and the transition rate from state 1 to 2 is defined as W_{12} , with A and B defined as the Einstein Coefficients.

$$W_{21} = B_{21}\rho(\nu) + A_{21} \quad (1)$$

$$W_{12} = B_{12}\rho(\nu) \quad (2)$$

It is further assumed that the atoms are in thermal equilibrium with a blackbody radiation field at temperature T. Therefore the energy density of the radiative field is given by the result obtained by Planck (Ref 9:104)

$$\rho(\nu) = \frac{8\pi n^3 h \nu^3}{c^3} \frac{1}{e^{h\nu/kT} - 1} \quad (3)$$

where n is the index of refraction of the medium and c is the velocity of light in a vacuum.

At thermal equilibrium, the number of 2 to 1 transitions must equal the number of 1 to 2 transitions in a given time interval so

$$N_2 W_{21} = N_1 W_{12} \quad (4)$$

where N_2 and N_1 are the number of atoms per unit volume in states 2 and 1 respectively.

Since the atoms are in thermal equilibrium, the ratio

N_2/N_1 is given by the Boltzman relationship

$$\frac{N_2}{N_1} = e^{-h\nu/kT} \quad (5)$$

Solving Eq (4) for N_2/N_1 and equating it to Eq (5) and substituting $\rho(\nu)$ from Eq (3) yields

$$\frac{8\pi n^3 h\nu^3}{c^3 (e^{h\nu/kT} - 1)} = \frac{A_{21}}{B_{12} e^{h\nu/kT} - B_{21}} \quad (6)$$

For this equality to hold, the following two Einstein relationships must hold (Ref 10:124)

$$B_{12} = B_{21} \quad (7)$$

$$\frac{A_{21}}{B_{21}} = \frac{8\pi n^3 h\nu^3}{c^3} \quad (8)$$

By solving Eq (8) for B_{21} (which equals B_{12} from Eq [7]) and substituting into Eq (2), the induced 2 to 1 (identical to the 1 to 2, transition rate then becomes

$$W_{12} = \frac{c^3}{8\pi n^3 h\nu^3 t_{\text{spon}}} \rho(\nu) \quad (9)$$

where $t_{\text{spon}} = 1/A_{21}$. This relationship holds for a uniform spectrum with energy density per unit frequency $\rho(\nu)$. From the standpoint of laser operation, transitions caused by single frequency radiation are of primary concern. If the induced transition rate for such transitions is denoted

$W_i(\nu)$, then

$$W_i(\nu) = \frac{c^3}{8 \pi n^3 h \nu^3 t_{\text{spon}}} g(\nu) \quad (10)$$

where $g(\nu)$ is the lineshape function of the transition.

In terms of intensity, I_ν , this becomes

$$W_i(\nu) = \frac{c^2 I_\nu}{8 \pi n^2 h \nu^3 t_{\text{spon}}} g(\nu) \quad (11)$$

If an atomic system with N_1 atoms per unit volume in state 1 and N_2 atoms per unit volume in state 2 is assumed, then the power generated per unit volume is

$$\frac{P}{\text{volume}} = (N_2 - N_1) W_i h \nu \quad (12)$$

Then, assuming no losses, the incremental increase in intensity dI_ν , per unit distance dz into the laser medium will equal the power generated per unit volume so from Eq (12)

$$\frac{dI_\nu}{dz} = (N_2 - N_1) W_i h \nu \quad (13)$$

and substituting Eq (11) into Eq (13) yields

$$\frac{dI_\nu}{dz} = (N_2 - N_1) \frac{c^2 I_\nu}{8 \pi n^2 \nu^2 t_{\text{spon}}} g(\nu) \quad (14)$$

The solution of Eq (14) is

$$I_\nu(z) = I_\nu(0) e^{\beta(\nu)z} \quad (15)$$

where the gain term

$$\beta(\nu) = (N_2 - N_1) \frac{c^2}{8 \pi n^2 \nu^2 t_{\text{spont}}} g(\nu) \quad (16)$$

It can be seen that when N_2 is greater than N_1 , that is when a "population inversion" exists, that the intensity of the radiation increases exponentially with the distance z into the medium. This is a prerequisite for the operation of any laser.

Emission and Absorption of Radiation in the Semiconductor

In a semiconductor, carrier (electron or hole) transitions occur between the conduction and valence bands. These bands are distributed in energy, unlike the atomic states (in solid state and gas lasers) which are characterized by well defined energy levels.

The goal of achieving stimulated emission in a semi-conductor laser is attained in a forward biased doubly degenerate p-n junction (Ref 8:177). A semiconductor is defined as degenerate when it is so heavily doped that the impurity concentration approaches, or is greater than the density of states (N_v or N_c) of the intrinsic material. When this is true, the Fermi Level lies in the conduction or valence band (Ref 11:151). (When the semiconductor is non-degenerate, the Fermi level lies in the energy gap). A doubly degenerate region in the p-n junction, then, is formed by heavily doping the n side of

the junction so that the Fermi Level lies in the conduction band and heavily doping the p side so that the Fermi Level lies in the valence band. Under steady state conditions (applied voltage equal to zero), these Fermi Levels must be aligned as shown in Fig. 2(a). When a forward bias (applied voltage approximately equal to E_g/e) is applied to the junction, the band structure changes as shown in Fig. 2(b). As a result of the applied voltage, there now exists a thin region in the semiconductor encompassing the junction, known as the "active region" or "recombination region," which is doubly degenerate and contains both electrons and holes. A unique characteristic of this process, not common to other lasers, is that the injected carriers (electrons or holes) contribute directly to replenishing the conduction and valence bands. The population inversion, then, is created directly by the injected current. The electrons from the conduction band of the n side are now free to recombine with the holes from the valence band of the p side in the active region resulting in the emission of light of frequency equal to E_g/h (Ref 13:25). When this process occurs inside an optical cavity, lasing action is sustained and the population inversion is maintained by the injected current.

An important consideration affecting this process is whether the semiconductor material has a direct or an indirect bandgap. When the conduction band energy minimum is aligned with the valence band energy maximum, as a function

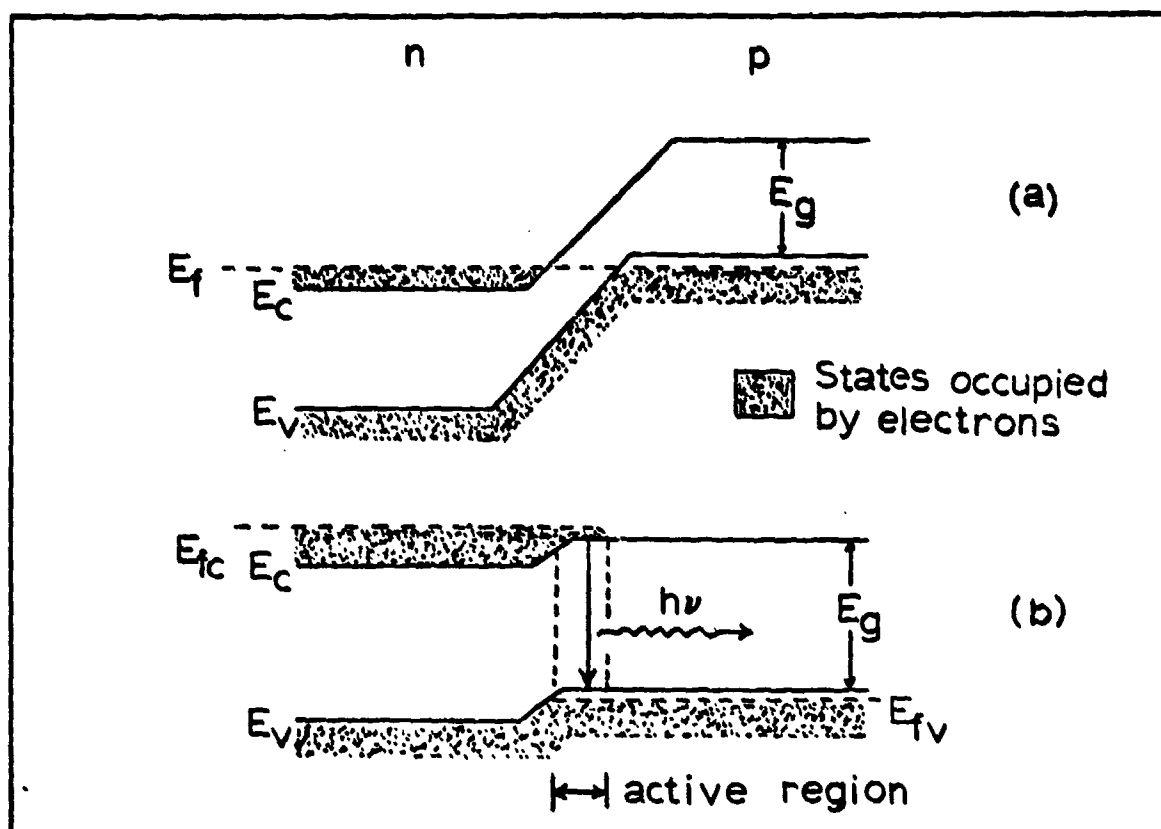


Fig. 2. Energy Band Diagram of Degenerate p-n Junction
(a) $V = 0$; (b) $V = E_g/e$ (Ref 12:24)

of momentum (Fig. 3[a]), the semiconductor is said to have a direct bandgap; when these points do not coincide, the semiconductor is said to have an indirect bandgap (Fig. 3[b]). In a transition such as that shown in Fig. 3(b), the emitted photon can account for only part of the large momentum change. Normally a phonon is emitted along with the photon to make up for the additional momentum, so that momentum is conserved in the process. Two undesirable results of this process, from the standpoint of efficiency, are that the phonon carries away a portion of the energy resulting from the transition and contributes to the internal heating of the junction region (Ref 13:204-207).

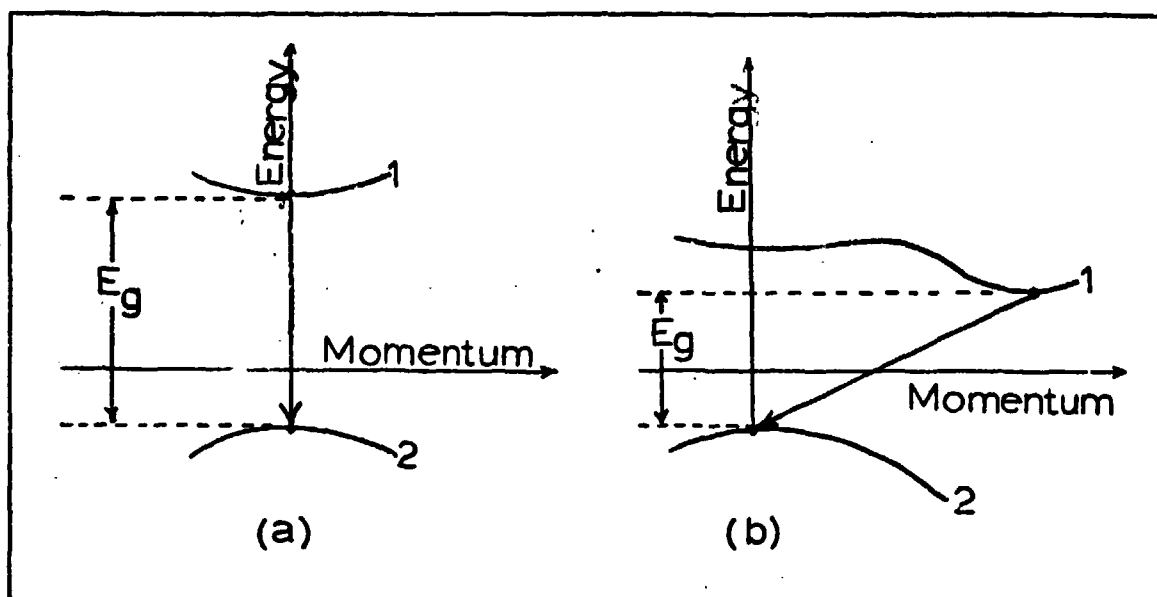


Fig. 3. Energy Band Diagram of (a) Direct Bandgap Material and (b) Indirect Bandgap Material (Line 1 represents the conduction band and line 2 represents the valence band.) (Ref 13:206)

If a junction with a mode volume described by $V = dLW$ is considered (Fig. 4), and the electron densities per unit volume in states 1 and 2 are substituted for the atom densities per unit volume in Eq (16), then the gain constant becomes

$$\beta(\nu) = \frac{(n_2 - n_1)}{dLW} \frac{c^2}{8\pi n^2 \nu^2 t_{recom}} g(\nu) \quad (17)$$

In most semiconductor lasers, the active region thickness, t , is less than the mode thickness, d . If, given a low temperature, and n_1 is assumed to be zero, then

$$\frac{n_2}{t_{recom}} = \frac{I \eta_i}{e} \quad (18)$$

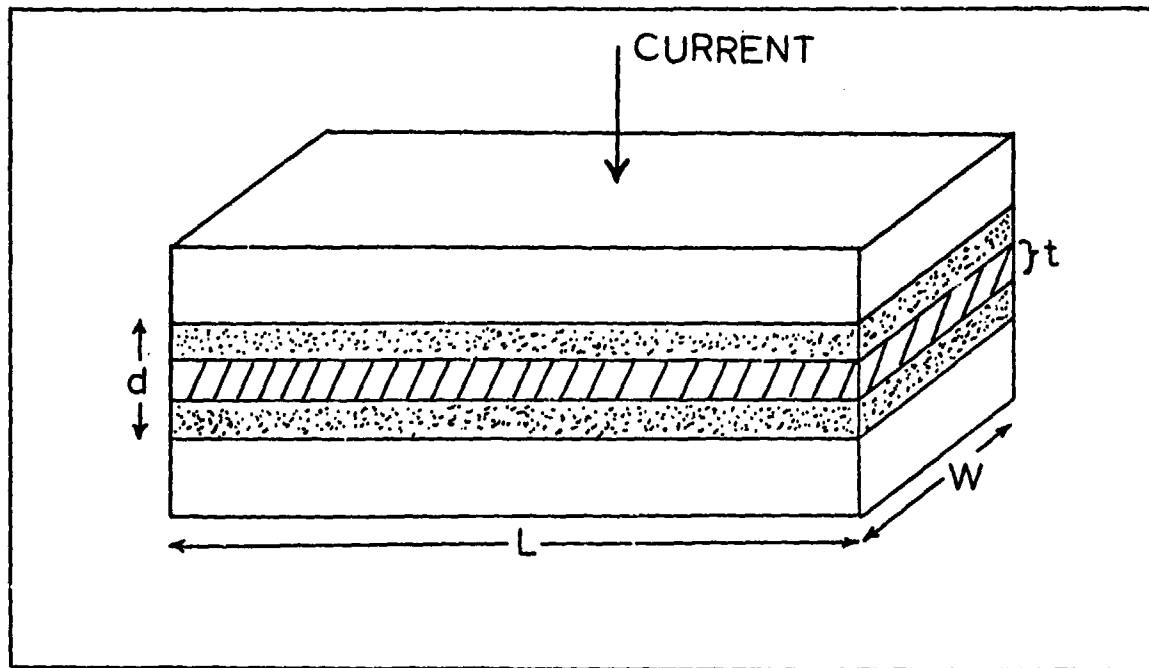


Fig. 4. Mode Volume (Product dLW) encompassing the optical mode emitted from a p-n junction with Carrier Recombination Region consisting of volume product tLW

where η_i is the internal quantum efficiency and I is the injected current.

Then, since $A = LW$, the cross sectional area for current flow

$$\beta(\nu) = \frac{c^2 g(\nu) \eta_i}{8 \pi n^2 \nu^2 e d} \left(\frac{I}{A} \right) \quad (19)$$

To determine the threshold for lasing, the expression $Re^{(\beta_t - \alpha)}$ is set equal to one (Ref 8:182), with β_t the gain factor at threshold, α the total internal loss term, and R the reflectivity such that $R = (r_1 r_2)^{1/2}$ with r_1 and r_2 the reflectivities of the cavity facets. Then from Eq (19)

$$\frac{I_t}{A} = \frac{8 \pi n^2 \nu^2 e d \Delta \nu}{c^2 \eta_i} \left[\alpha - \frac{1}{L} \ln (R) \right] \quad (20)$$

where I_t is the threshold current for lasing. Substituting $\Delta \nu = \Delta E/h$ and $\nu = c/\lambda$ yields

$$J_t = \frac{8 \pi n^2 e^2 d \Delta E}{\lambda^2 h \eta_i} \left[\alpha + \frac{1}{L} \ln \left(\frac{1}{R} \right) \right] \quad (21)$$

where J_t is the threshold current density, λ is the wavelength of the radiation, and ΔE is the linewidth of the spontaneous radiation in electron volts. A more rigorous treatment of the threshold current density by Casey and Panish (Ref 33:181-183) and Stern (Ref 14:437) includes a factor γ in the expression for J_t so that

$$J_t = \frac{8 \pi n^2 e^2 d \Delta E \gamma}{\lambda^2 h \eta_i} \left[\alpha + \frac{1}{L} \ln \left(\frac{1}{R} \right) \right] \quad (22)$$

Further analysis of γ , other than to state that it is a function of temperature and doping, is beyond the scope of this thesis. γ has been tabulated by Stern (Ref 14:438) for different values of doping and temperature.

Output Power of the Semiconductor Laser

The power emitted by a semiconductor laser as a result of stimulated emission is (Ref 8:185)

$$P = \frac{(I - I_t) \eta_i h \nu}{e} \quad (23)$$

where η_i is the internal quantum efficiency of the device. The fraction of this power that is realized as output is determined by the total internal absorption of the device α , and the ratio $(1/L)\ln(1/R)$, which will be referred to later in this thesis as parameter C. The output power P_{out} then becomes (Ref 8:185)

$$P_{out} = \frac{(I - I_t) \eta_i h\nu}{e} \left(\frac{(1/L)\ln(1/R)}{\alpha + (1/L)\ln(1/R)} \right) \quad (24)$$

or

$$P_{out} = \frac{(I - I_t) \eta_i h\nu}{e} \left(\frac{C}{\alpha + C} \right) \quad (25)$$

III. The Semiconductor Laser

The various types of semiconductor lasers will be discussed in this section. Some of the different methods of laser fabrication will be discussed briefly. Finally, the different types of optical cavities will be presented. The discussion of semiconductors in this section will be limited to those made of GaAs and its compounds.

The Homojunction Laser

The first successful semiconductor lasers were homojunction devices, developed in 1962 by Nathan et al. (Ref 15), Quist et al. (Ref 16), Hall et al. (Ref 17), and Holonyak et al. (Ref 18). The homojunction laser is so called because it is made from a single piece of semiconductor material. The usual method of forming the junction is by diffusing an acceptor element such as Zinc into a GaAs substrate, which has been doped negatively with an element such as Selenium. A small volume enclosing the resulting p-n junction is called the "active region." It is here that the lasing action takes place. The radiation from the device is emitted from the active region parallel to the plane of the junction as shown in Fig. 5.

The Heterojunction Laser

The first heterojunction laser was proposed by Kroemer in 1963 (Ref 20). The heterojunction laser is so

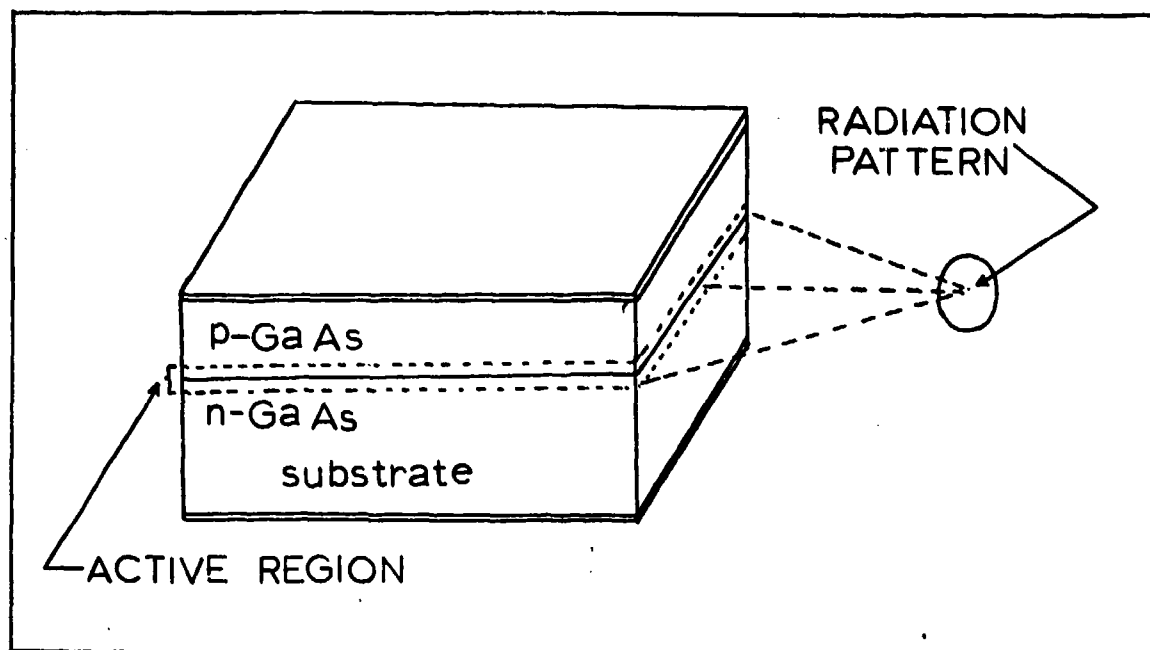


Fig. 5. Typical Homojunction Laser (Ref 19:1513)

called because the device consists of several layers of semiconductor materials, which are normally, epitaxially grown solid solutions such as $\text{Al}_x\text{Ga}_{1-x}\text{As}$ (Fig. 6). The principal advantage of the heterojunction laser over the homojunction laser is that the carriers (electrons and holes) and the optical mode can be more efficiently confined to a definite volume bounded by the heterojunctions. This results in decreased losses of both carriers and radiation to the area surrounding the active region. The percentage of Aluminum present in a layer is normally indicated by a variable x , y , or z contained in the expression for the chemical compound. For example, $\text{Al}_x\text{Ga}_{1-x}\text{As}$ contains an x fraction of Aluminum and a $(1-x)$ fraction of Gallium. Two very important parameters of the compound can be altered by changing the variable x .

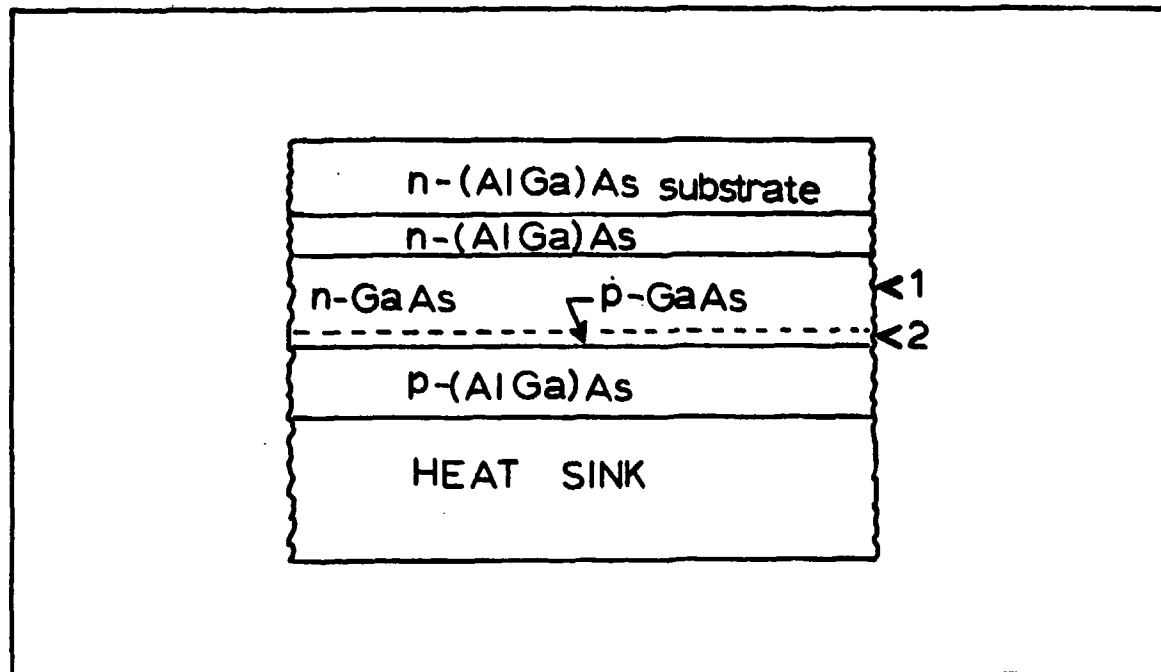


Fig. 6. Large Optical Cavity Heterostructure Laser proposed by Lockwood et al. (1)--Optical Cavity; (2)--Recombination Region (Ref 22:499)

The index of refraction n , can be varied from 2.9 for AlAs ($x = 1$) to 3.6 for GaAs ($x = 0$) (Ref 21:463). The energy bandgap, E_g , varies from a direct gap of 1.424 eV for GaAs ($x = 0$) to an indirect gap of 1.92 eV for $\text{Al}_{0.37}\text{Ga}_{0.63}\text{As}$ to an indirect gap of 3.1 eV for AlAs ($x = 1$) (Ref 19:1512-1514).

Several types of heterojunctions have evolved from the original concept. The Single Heterostructure (SH) laser contains only one heterojunction so that the radiation is confined at only one boundary. The Double Heterostructure (DH) laser contains two heterojunctions such that the carriers and radiation are bounded on both sides of the active region. The Separate Confinement Heterostructure (SCH) laser is characterized by confinement of the carriers to a

restricted region within the optical cavity (Ref 19:1521-1527). The Large Optical Cavity (LOC) laser described by Lockwood et al. (Ref 22) is a typical example of the SCH laser, since it consists of a very thin active region (less than 1 micrometer) located in a relatively thick (several micrometers) optical cavity (Fig. 6). More sophisticated versions of the SCH laser, which have been developed recently are the Ternary Heterostructure (TH) and Quaternary Heterostructure (QH) lasers. These devices have additional layers of $\text{Al}_y\text{Ga}_{1-y}\text{As}$ bounding the active region, resulting in even more efficient confinement of the radiation (Ref 6:9-11). A schematic diagram of typical SH, DH, TH, and QH lasers with a qualitative representation of the relative bandgap E_g , and index of refraction n , for each laser is depicted in Fig. 7.

The fabrication of heterojunction lasers was made possible by the development of several crystal growth processes. The most common ones are Liquid Phase Epitaxy (LPE), Vapor Phase Epitaxy (VPE), Molecular Beam Epitaxy (MBE), and Metal Organic Chemical Vapor Deposition (MOCVD). LPE is currently the most widely used technique of these. LPE and VPE are accomplished by the growth of successive layers of GaAs and $\text{Al}_x\text{Ga}_{1-x}\text{As}$ onto the (100) crystallographic surface of a GaAs substrate. The layers are grown by bringing the different solutions into contact with a seed, while cooling (Ref 19:1513). Lattice matching of the different layers is very important and is readily accomplished since

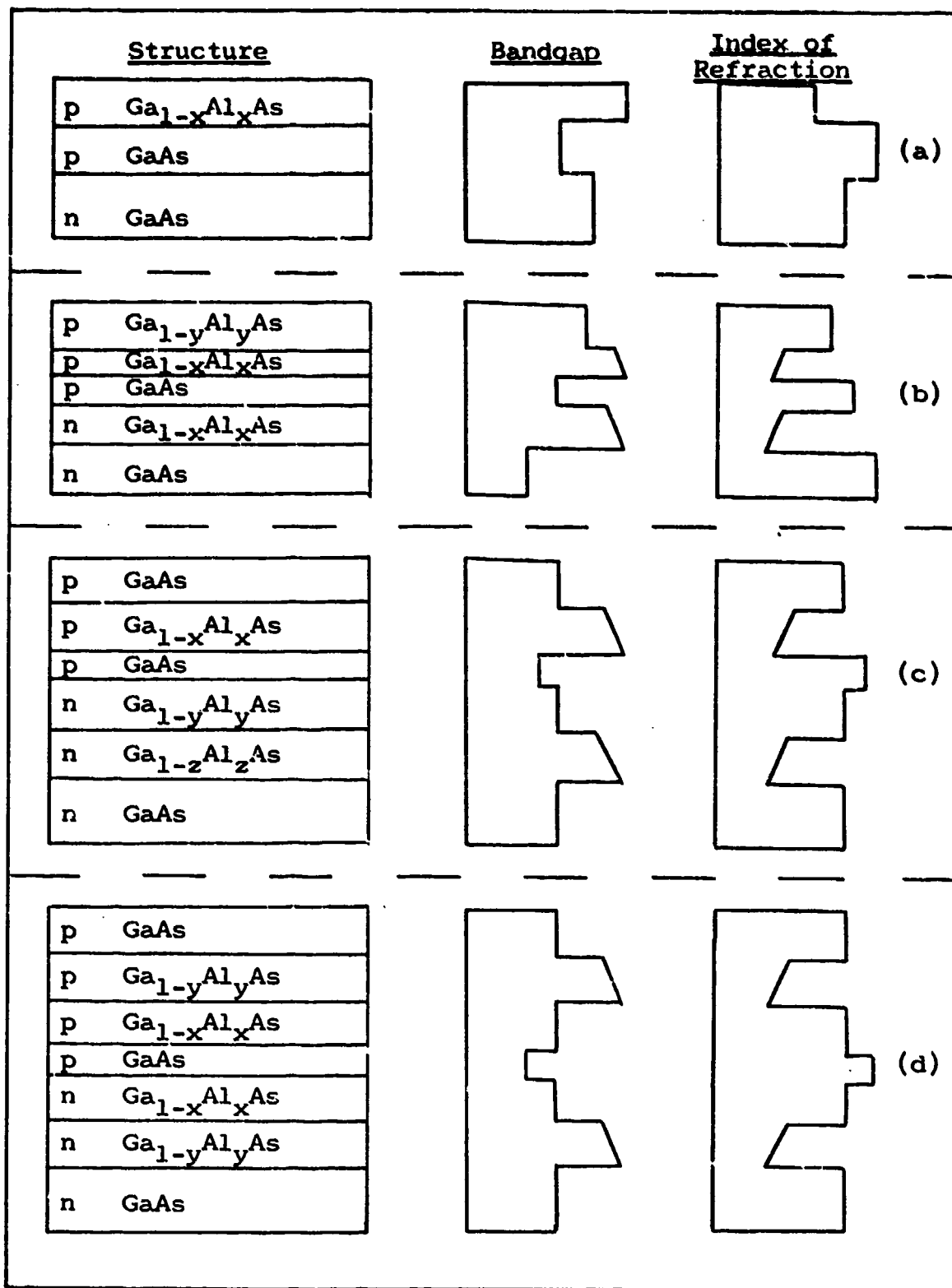
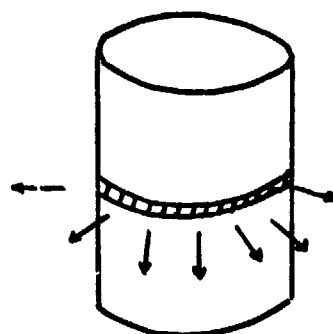


Fig. 7. Typical Heterostructure Lasers with a qualitative representation of bandgap, E_g , and index of refraction, n . (a) SH Laser ($x=0.07$); (b) DH Laser ($x=0.30$, $y=0.00$); (c) TH Laser ($x=0.40$, $y=0.03$, $z=0.10$); (d) QH Laser ($x=0.25$, $y=0.04$) (Ref 6:7-11)

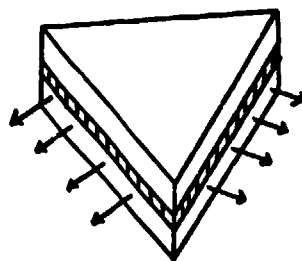
the lattice parameters of 5.6535 Angstroms for GaAs and 5.6390 Angstroms for AlAs are very close (Ref 21:457). MBE and MOCVD are relatively new techniques. MBE is accomplished by directing a beam of Gallium, Aluminum, and dopant atoms and Arsenic molecules onto a heated substrate of GaAs under very high vacuum conditions (Ref 19:1514). Successful operation of DH lasers prepared by this technique has been achieved by Cho et al. (Ref 23). The first successful growth of an AlGaAs/GaAs DH laser entirely by MOCVD was reported by Dupis and Dapkus in 1977 (Ref 24). The principal advantage of this technique over the others is that large area (greater than 12 cm^2) layers of $\text{Al}_x\text{Ga}_{1-x}\text{As}$ can be uniformly grown (Ref 24:466). In all of these methods, the growth of the layers on the substrate, oriented in the (100) direction, permits cleaving the wafer in the (110) direction. Cleaving the wafer in this direction provides the reflecting facets needed to form the Fabry-Perot cavity, which will be discussed in the next section.

The Optical Cavity

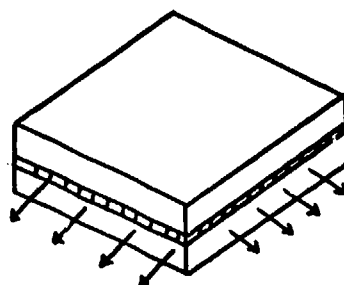
There is a wide variety of optical cavities in which the lasing process can be sustained. The three major geometrical arrangements, shown in Fig. 8 are the circular, triangular, and rectangular (Ref 11:701). There are two types of rectangular cavities. One has four sides of the rectangle polished, so that the radiation is emitted in four directions. The other type has two opposing sides polished and the remaining two sides roughened (normally 1



(a)



(b)



(c)

Fig. 8. Optical Cavities Other Than Fabry-Perot: (a) Circular, (b) Triangular, (c) Rectangular (Four sides polished)
(Ref 11:701)

cutting with a saw or by proton bombardment). The type with two polished sides is called the Fabry-Perot cavity and is the most widely used of all cavity designs today for semiconductor lasers (Fig. 9).

It is difficult to obtain a single stable longitudinal mode from the conventional Fabry-Perot cavity, particularly at high operating currents (Ref 19:1529-1530). In 1971 Kogelnik and Shank introduced the concept that the Fabry-Perot mirrors could be replaced by a feedback mechanism provided by Bragg scattering from a grating within the lasing medium (Ref 25). Lasers with this type of cavity have come to be known as Distributed Feedback (DFB) lasers. A typical DFB device is depicted in Fig. 10 (Ref 26:123).

Finally, a ring laser recently operated successfully by Matsumoto and Kumabe (Ref 27), is shown in Fig. 11. However, the design of an output coupler is necessary before the radiation can be extracted from this device.

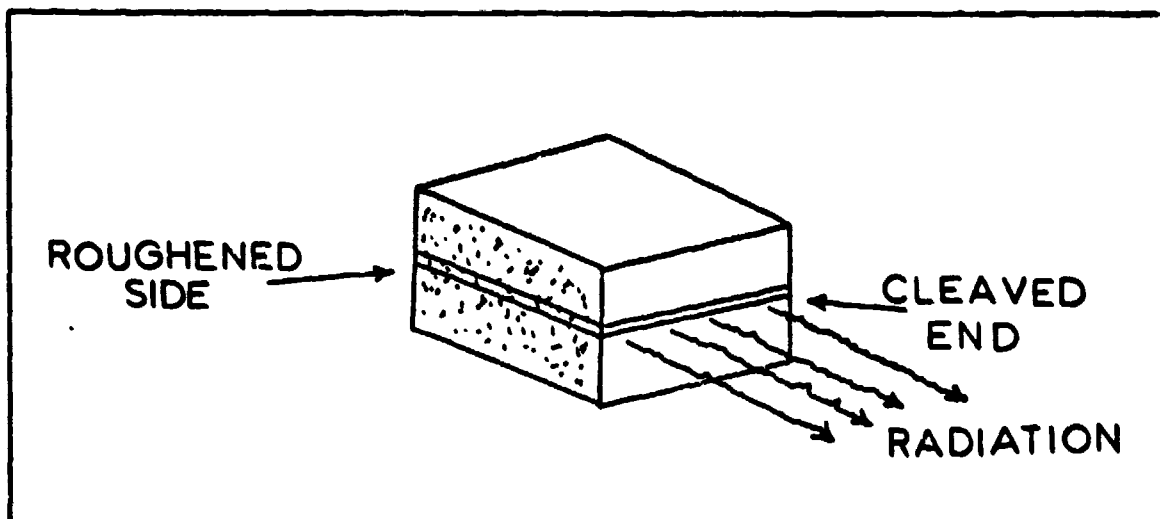


Fig. 9. Typical Fabry-Perot Cavity

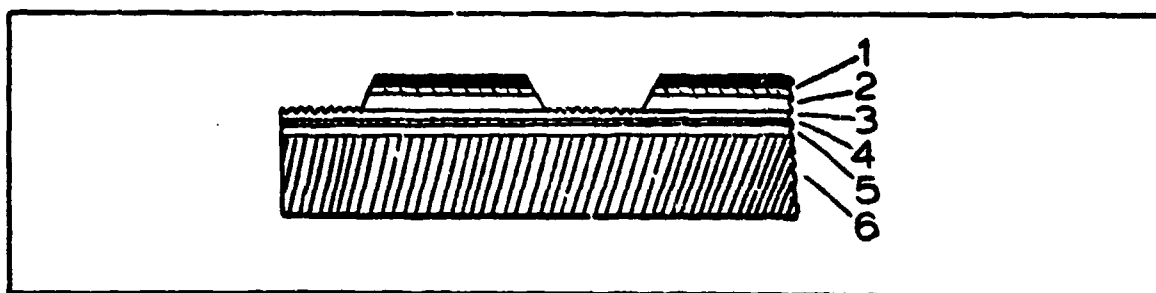


Fig. 10. Typical Distributed Feedback Laser: (1) p-GaAs; (2) p-Ga_{0.65}Al_{0.35}As; (3) p-Ga_{0.85}Al_{0.15}As; (4) p-Ga_{0.95}Al_{0.05}As; (5) n-Ga_{0.65}Al_{0.35}As; (6) n-GaAs (Ref 26:123)

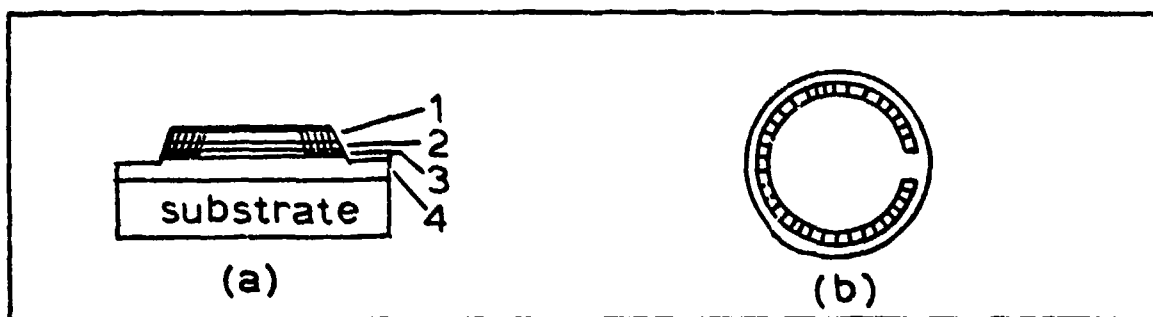


Fig. 11. Typical Ring Laser (Ref 27:1396)

IV. Optimization of the Laser Design for Maximum Output Power

The basic theory governing the operation of the semiconductor laser has been presented; and, the various types of devices which have been successfully operated based on this theory have been described. In this section, this information will be analyzed to determine which type of laser design will provide the device capable of yielding the maximum continuous wave, output power.

The Material

Gallium Arsenide has been selected as the basic laser material for the purpose of this thesis. The principal motivation for this choice was to reduce the number of variables in the overall problem of optimizing output power, by starting with a material about which a substantial amount of information was currently available. Gallium Arsenide has been the most popular candidate, to date, for development, primarily because it is a direct bandgap material. Indirect bandgap materials are not suitable for development as high power CW devices due to the fact that phonons are normally emitted along with the photons during electron transitions, as discussed in Chapter II. These phonons contribute to internal heating in the semiconductor limiting the maximum power obtainable from the device. Also, the

electron transitions resulting in stimulated emission have a greater probability of occurrence in direct bandgap materials than in those with an indirect bandgap. Therefore, greater total amplification of the radiation and consequently, greater output power will result in lasers made from a direct bandgap material (Ref 12:15-16). Although the ideas presented in this chapter are based on the specific characteristics of GaAs, they should be applicable to other Group III-V compounds. It should be noted, however, that the thermal conductivity of Group III-V ternary compounds (e.g., $\text{Al}_x\text{Ga}_{1-x}\text{As}$) and quaternary compounds (e.g., $\text{In}_x\text{Ga}_{1-x}\text{As}_y\text{P}_{1-y}$) is substantially lower than that of the pure materials (Ref 28:1293). Thermal conductivity is an important parameter in the design of a CW laser and will be discussed in Chapter V.

The Cavity

The Fabry-Perot rectangular optical cavity (Fig. 9) has historically been the most practical and efficient cavity for the semiconductor laser. The principal advantage of this design is that the parallel reflecting facets can be conveniently formed by cleaving the GaAs crystal along the (110) crystallographic plane. The sides of the cavity are normally roughened by sawing.

Optimization of the Cavity Dimensions

In Chapter II, an expression for the total output power of a semiconductor was presented

$$P_{out} = \frac{(I - I_t) \eta_i h \nu}{e} \left(\frac{(1/L) \ln(1/R)}{\alpha + (1/L) \ln(1/R)} \right) \quad (24)$$

where from Eq (22)

$$I_t = (LW) \frac{8 \pi n^2 e^2 d \Delta E \gamma}{\lambda^2 h \eta_i} [\alpha + (1/L) \ln(1/R)] \quad (26)$$

In this section, Eq (24) will be analyzed to determine how the variables L, W, and d affect P_{out} and how these variables may be optimized to achieve the maximum output power. Two important assumptions have been made to accomplish this. First, thermal effects, as a result of junction heating, have been neglected (this topic will be discussed in Chapter V). Second, a constant absorption coefficient α , is assumed (absorption effects will be discussed in the next section). The following typical experimental values of GaAs lasers will be assumed for the purposes of the computations in this section: $T_{heat\ sink} = 77K$; $\eta_i = 1$; $\lambda = 0.84 \times 10^{-6}m$; $\nu = 3.571 \times 10^{14}Hz$; $n = 3.6$; $\Delta E = 0.025eV$ (Ref 21:438); $\gamma = 3.1$ (Ref 21:438); and $\alpha = 6\ cm^{-1}$.

A uniform current density $J = 10,000\ A/cm^2$ is assumed in a device of thickness $d = 0.0001\ cm$ and reflectivity $R = 0.30$. A plot of P_{out} against cavity length L, for cavity widths W of 0.005, 0.010, 0.015, and 0.020 cm, was obtained using Eq (24), and is shown in Fig. 12. It can be seen in general, that increasing the cavity dimensions L and W will provide a device with greater output power;

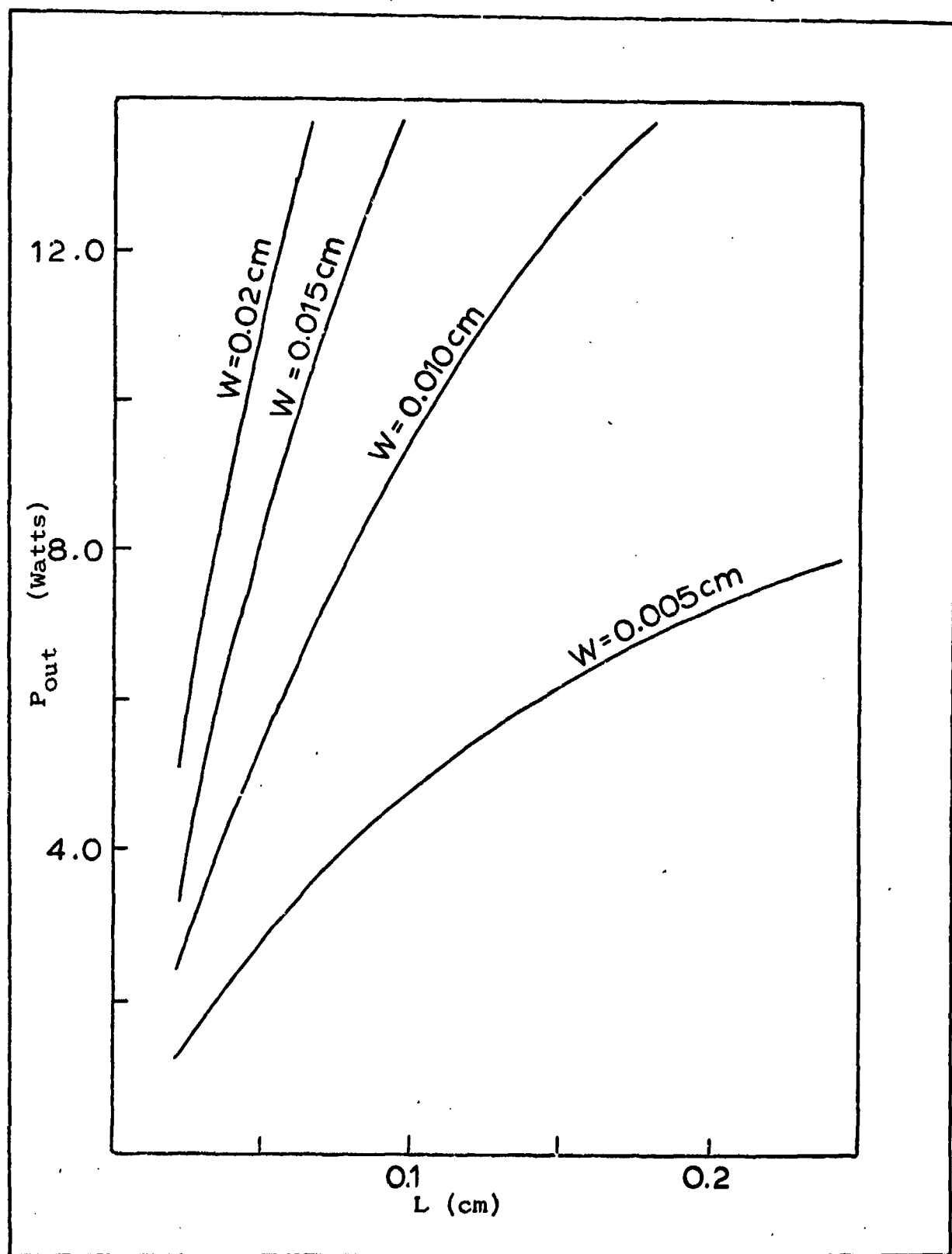


Fig. 12. Output Power vs Cavity Length for Different Values of Cavity Width ($d = 0.0001 \text{ cm}$; $R = 0.30$; $J = 10,000 \text{ A/cm}^2$)

although the device may not necessarily be operating at its maximum possible external quantum efficiency.

Assuming a constant absorption coefficient, it is theoretically possible to maintain a constant external quantum efficiency, η_{ext} , while changing the cavity length L . η_{ext} is defined as the ratio of the photon output rate (due to an increase in injected current) to the increase in injected current (Ref 8:186), and

$$\eta_{\text{ext}} = \frac{\eta_i}{1 + [\alpha L / \ln(1/R)]} \quad (27)$$

This can be accomplished by maintaining the parameter $1/C$, which appears in Eq (27), at a constant value. C was previously defined

$$C = (1/L) \ln(1/R) \quad (28)$$

If C is fixed, then for every value of L , there exists (at least theoretically) a corresponding value of R . It should be noted that parameter C appears in both Eq (24) and Eq (26).

A uniform current density $J = 10,000 \text{ A/cm}^2$ is again assumed in a device of thickness $d = 0.0001 \text{ cm}$, but the reflectivity R is now altered with each value of cavity length to maintain a constant value of 30 cm^{-1} for parameter C . P_{out} is plotted against L (with corresponding values of R) for cavity widths of 0.005, 0.010, 0.015, and 0.020 cm in Fig. 13. There is a marked increase in output power for a given length, compared to the values shown in Fig. 12. This increase is most pronounced for values of W which are small compared to L , that is when the ratio W/L

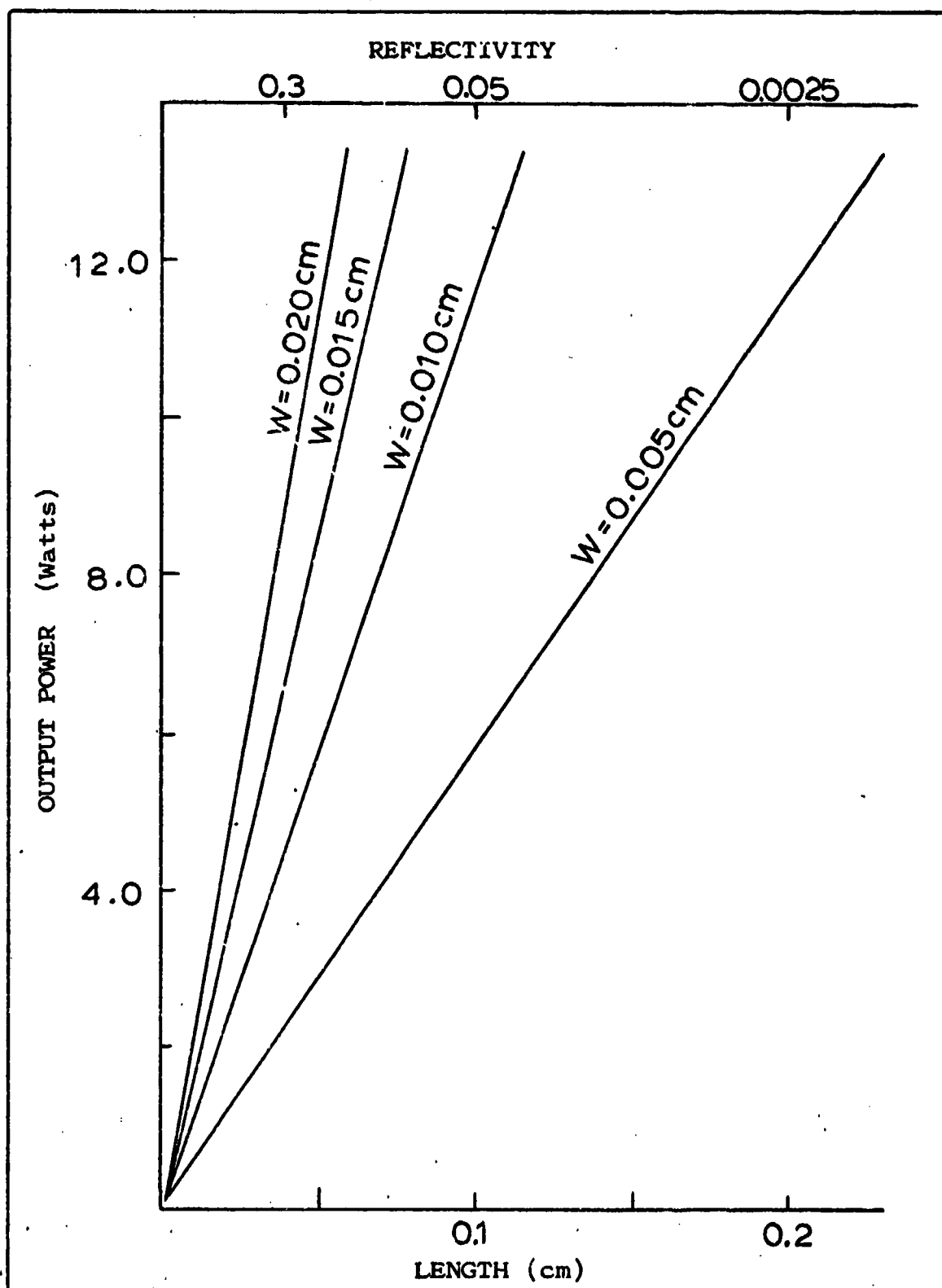


Fig. 13. Output Power vs Length and Reflectivity for Different Values of Width ($d = 0.0001 \text{ cm}$; $C = 30.0 \text{ cm}^{-1}$; $J = 10,000 \text{ A/cm}^2$; $J_t = 500 \text{ A/cm}^2$; $\eta_{\text{ext}} = 0.83$)

is much less than unity, which would be the case in a device with realistic dimensions.

The normal reflectivity for a GaAs - air interface is between 0.25 and 0.30. This reflectivity can be decreased through the use of antireflective coatings. A study of the effects of antireflective coatings by Ulbrich and Pilkuhn was accomplished in 1970. In this study, R was varied between values of 0.25 and 0.03 (for an air interface) (Ref 30:314), and the results obtained agreed with those predicted by Eq (27) for different values of R (Ref 30:315). Consequently, the feasibility of reducing the reflectivity of the cavity facet, to values in the neighborhood of 0.03 has already been demonstrated.

Another important consideration that will affect the laser performance is, that for lasing to occur within the optical cavity, the condition necessary for the propagation of a standing wave specified by

$$\lambda q = 2Ln \quad (29)$$

must be satisfied (Ref 13:73), where q is an integer. Although the results of this section indicate that increasing L will result in increasing P_{out} , it is important to note that if Eq (29) is not satisfied, the laser may not operate at all.

Although a thorough analysis of mode generation and interaction within the optical cavity is beyond the scope of this thesis, it is important at this point to briefly

discuss the effect of internal circulating modes on the laser operation. In experiments with dual cavity lasers, Ettenberg et al. have observed that the existence of internal circulating modes results in an abrupt decrease in the external quantum efficiency of the device, since a substantial portion of the radiation is lost out the sides of the cavity. Special cutting or sawing of the sidewalls of the Fabry-Perot cavity will generally suppress these modes, but this approach is not always practical (Ref 31:5049). These modes can also be suppressed by careful selection of the laser length to width ratio. Ettenberg et al. determined that for a uniformly pumped semiconductor, the onset of internal circulating modes will be prevented when

$$\left(\frac{0.275}{W} \ln G \right) > \left(\frac{1}{L} \ln \frac{1}{R} \right) \quad (30)$$

where G is a constant dependent on the scattering losses at the sawed sidewall of the cavity (Ref 31:5050).

The last parameter to be considered in this section is the cavity thickness d . The P_{out} is plotted as a function of d in Fig. 14. It is clear from this figure and from Eq (24) that P_{out} will increase linearly with decreasing d . Although Eq (24) predicts that this increase in P_{out} is linear for all d , experiments have shown that if d is decreased below some critical thickness (near $0.1 \times 10^{-6}m$), there is a sharp drop in P_{out} and a corresponding rapid rise in J_t (Ref 32:2093). It is believed that this is due

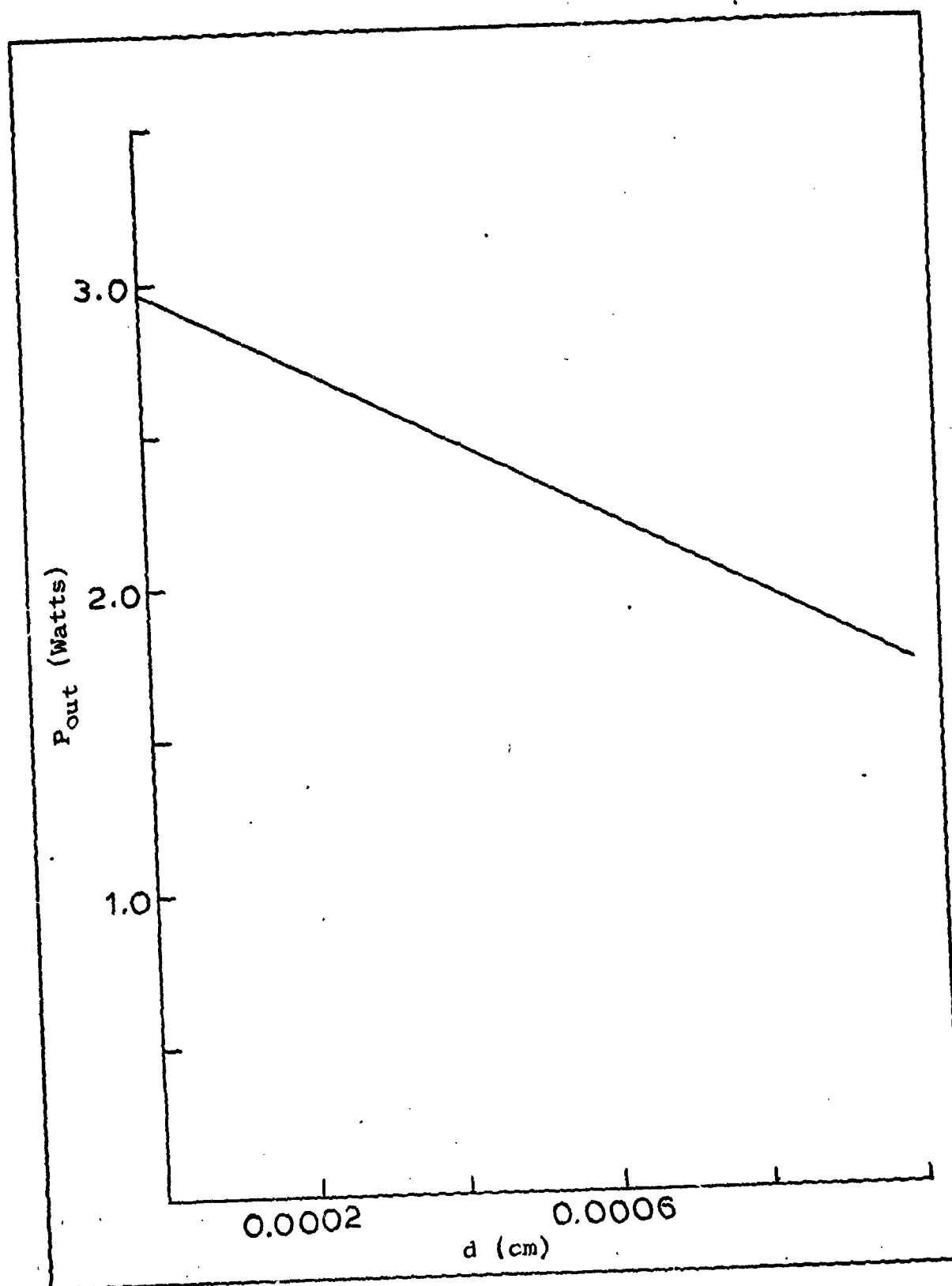


Fig. 14. Output Power vs Cavity Thickness ($L = 0.05$ cm;
 $W = 0.005$ cm; $R = 0.30$; $J = 10,000$ A/cm²)

to the fact that the optical cavity is too thin to accommodate the entire optical mode (Ref 19:1521).

Internal Absorption and Diffraction Effects

The absorption coefficient, α , includes all internal loss factors in the laser. There are three important loss factors which contribute to α . The free carrier absorption α_{fc} , as the name implies, is a result of nonradiative recombination of injected carriers with electrons or holes in the semiconductor. The scattering α_s , is caused by irregularities at the boundaries of the optical cavity, and at impurity centers in the semiconductor, resulting in less than 100 percent confinement of the optical mode (Ref 33: 174-175). Finally, the diffraction loss, α_D , occurs due to the fact that not all of the radiation, which is reflected by one of the laser facets, is incident on the facet at the opposite end of the laser. Some of the radiation is diffracted into the surrounding layers of the laser.

Results from experiments with homostructure lasers in the mid 1960s indicated that the total internal absorption of a semiconductor increased in proportion to the laser length, resulting in a corresponding decrease in the external quantum efficiency of the device (Ref 34:173). More recent studies of heterostructure lasers indicate that the opposite is true. In 1971, Adams and Cross predicted that the absorption coefficient was inversely proportional to L (Ref 35:878). This prediction was based on a solution of

the wave equation for an electromagnetic wave propagating in the center layer of a three-layer dielectric waveguide. This model closely approximates the situation existing in a heterostructure laser. Experimental data obtained by Goodwin and Selway for a heterostructure laser are in close agreement with this theory (Ref 36:289). A plot of the theoretical and experimental diffraction loss as a function L is shown in Fig. 15 (Ref 35:878).

Again using Eq (24), and including the experimental values for $\alpha(L)$ from Fig. 15, assuming a constant current density $J = 10,000 \text{ A/cm}^2$ in a device of thickness $d = 0.0001 \text{ cm}$, and varying the reflectivity with length as in Fig. 13, P_{out} is plotted as a function of L in Fig. 16. It can be seen that when the absorption coefficient is greater than 6 cm^{-1} (assumed in Fig. 13) for small L , the output power is slightly lower and when the absorption coefficient is less than 6 cm^{-1} , for large L , then the output power is slightly higher for a given length compared to Fig. 13.

Until recently, it was generally assumed that absorption was only a weak function of temperature, particularly at low temperatures (Ref 37:565). However, a recent (1978) study by Hwang et al. indicates that α is a very sensitive function of temperature down to 10K (Ref 38:32). This dependence must be due primarily to the contribution from α_{fc} , since as temperature decreases, fewer thermally excited carriers are available.

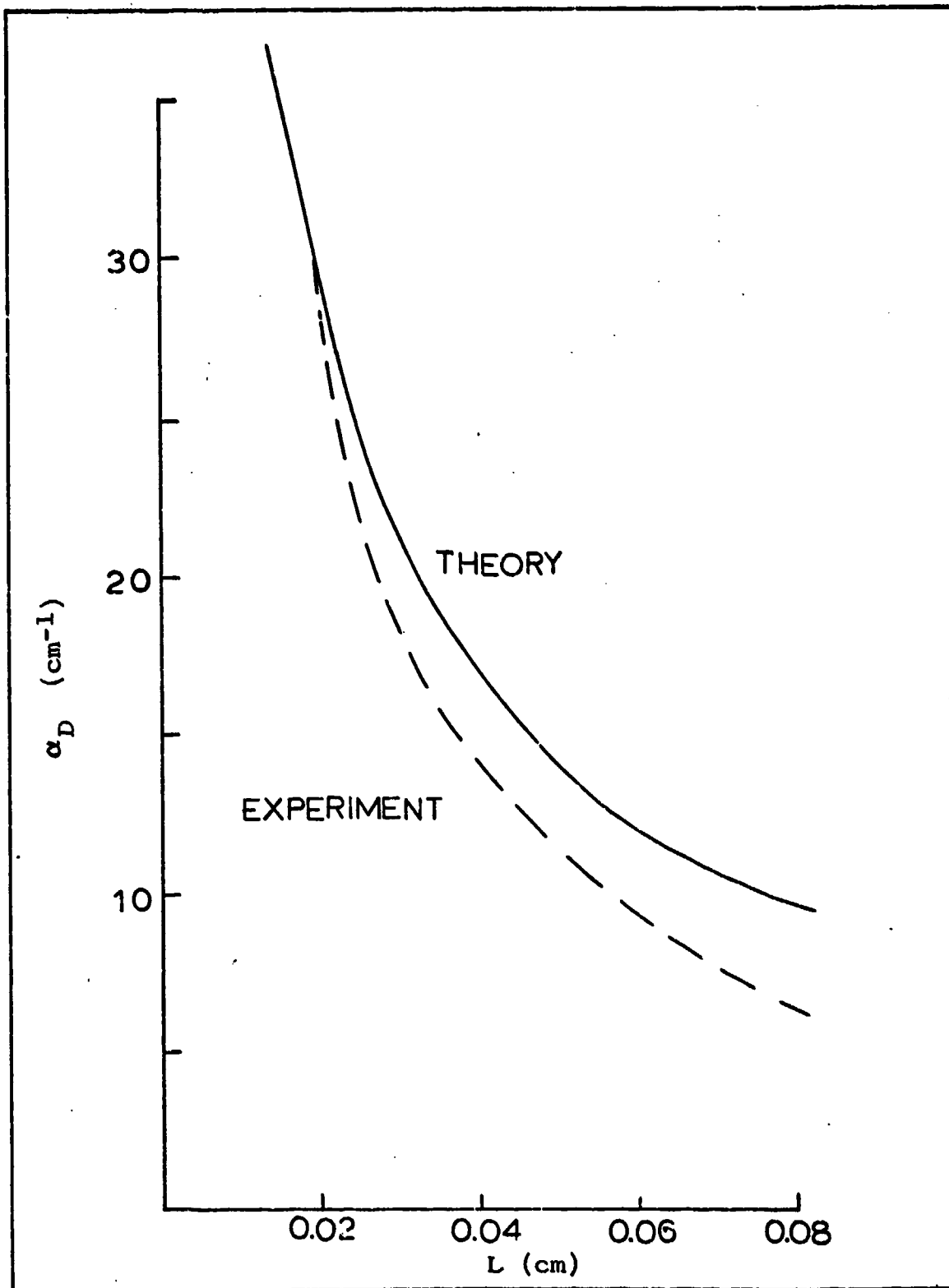


Fig. 15. Theoretical (Ref 35:878) and Experimental (Ref 36:289) Absorption Due to Diffraction vs Laser Length for SH laser ($\text{Al}_{0.4}\text{Ga}_{0.6}\text{As}$; $d = 1.6$ micrometers; $\gamma = 1$).

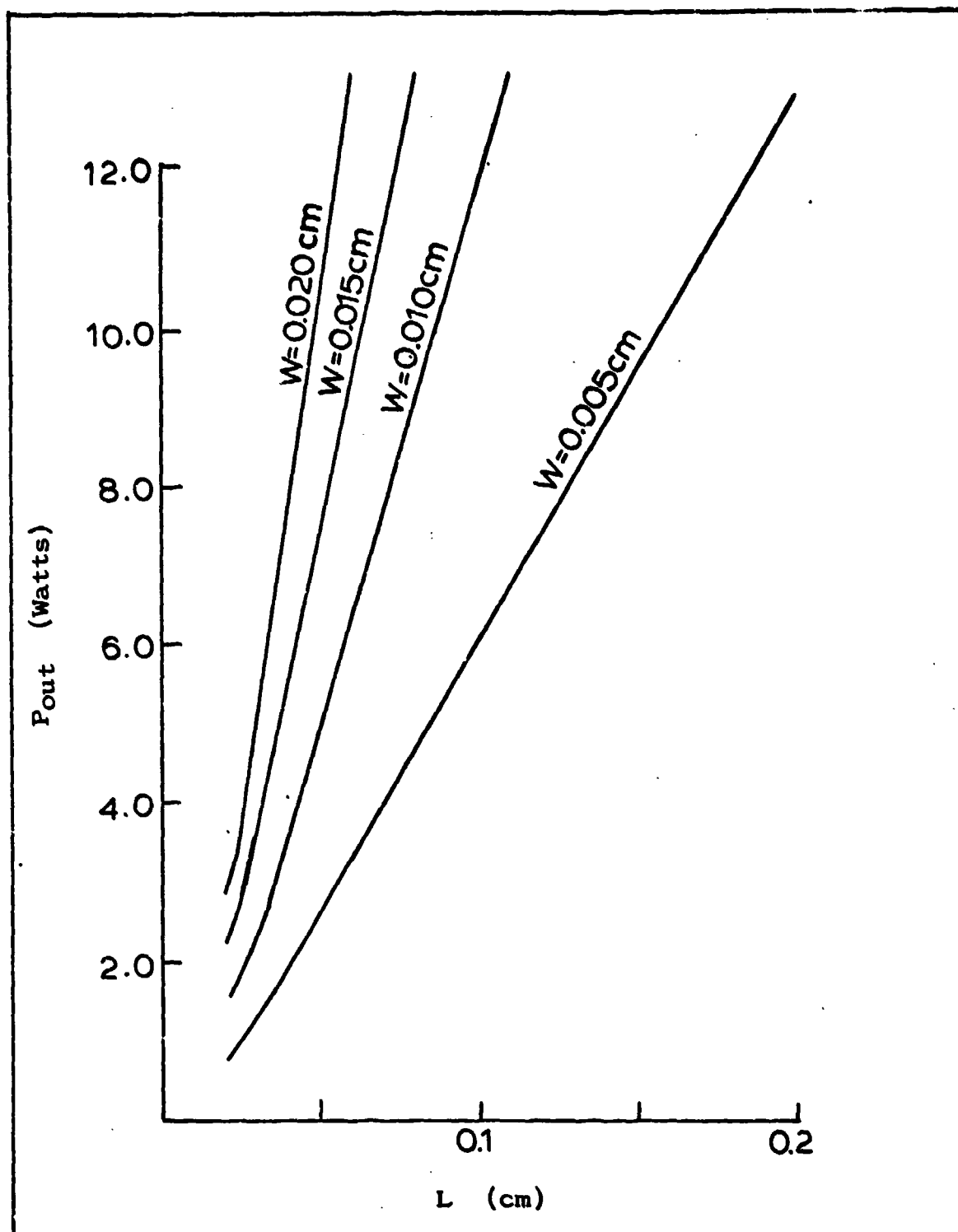


Fig. 16. Output Power vs Laser Length for Different Values of Width With Values of α from Fig. 15 ($d = 0.0001 \text{ cm}$; $C = 30 \text{ cm}^{-1}$; $J = 10,000 \text{ A/cm}^2$; $J_t = 500 \text{ A/cm}^2$; $\eta_{ext} = 0.83$)

The Laser Structure

The results of the previous section indicate that the output power of a semiconductor laser can be dramatically increased by increasing the laser length and width and maintaining a small d .

The Homojunction (diffused junction) Laser is not a suitable structure for implementing these results, primarily because a small optical cavity thickness with definite geometrical boundaries does not exist in this structure. In addition, internal absorption of the optical mode in the regions bordering the active region is very high for the homojunction laser compared to the epitaxially grown heterostructure devices. The slope of the power curves in Figs 12, 13, and 16 would be substantially smaller for homojunction lasers, since the internal absorption in these devices, due to inefficient mode confinement, would increase markedly with increasing length and become the driving function of Eq (27).

The heterojunction lasers on the other hand, provide excellent confinement of the optical mode to a waveguide with definite geometrical boundaries formed by the heterojunctions. Of the heterostructures presented in Chapter III, the Double Heterostructure laser theoretically appears to be the structure capable of producing the highest output power, since it is characterized by a very small d . However, an important phenomenon called "catastrophic degradation," discussed in the Appendix, must be considered at

this point. If the optical energy flux density exceeds a certain value at the output facet of the laser, the laser will fail catastrophically. This flux density can be reduced by increasing the area of the output facet. A larger output facet area can be obtained by increasing d . Increasing d , while maintaining t constant can be achieved best in the LOC heterostructure laser proposed by Lockwood et al. (Fig. 6) (Ref 22). The major advantage of the LOC laser is that the carriers can be confined to a narrow region within the optical cavity. The thickness t , of this carrier recombination region, must be much smaller than the minority carrier diffusion length, so that uniform excitation is achieved in this region (Ref 34:1281). Since the minority carrier diffusion length in GaAs, for typical doping levels, is of the order of a few micrometers (Ref 19:1513), maintaining the thickness t of the recombination region near 1 micrometer results in a device with a low J_t and a high internal quantum efficiency. This is accomplished in the LOC laser by proper selection of the Aluminum content in the layers bounding the recombination region. If t is reduced below some critical thickness t' , J_t increases sharply (Ref 19:1521). This t' is dependent on temperature and doping and is normally of the order of 0.2 micrometers (Ref 19:1523).

Lockwood et al. demonstrated that lasers with optical cavities as thick as 30 micrometers could be successfully operated (Ref 22). A large cavity thickness is feasible in

these devices due to the fact that the radiation propagates primarily in the n-type GaAs, which comprises the major portion of the optical cavity (Ref 22:500). The absorption coefficient in this medium is significantly lower than in p-type compensated GaAs or in AlGaAs (Ref 22:500,502). It should be possible to obtain a high power CW output from such a device if it is cryogenically cooled by a heat sink. In order to achieve the minimum junction to heat-sink distance, for most efficient cooling, Kressel et al. recommend mounting the device on the heat sink with the p-side down as shown in Fig. 6 (Ref 37:566).

Stripe Geometry

Many GaAs heterostructure lasers have recently been designed implementing "stripe geometry" (Refs 39; 40; 41). In these devices a narrow stripe (usually 10-15 micrometers wide) is formed on the top of the laser, normally through insulation by SiO_2 (Ref 42:94) or SiO (Ref 43:987) as shown in Fig. 17. The three main advantages of this design are: (1) Laser emission can be effectively limited to the single dominant mode; (2) the total operating current of the device is less for a given current density, since the current is spread over a smaller cross-sectional area; and, (3) degradation, due to the edge effects near the "sawed" sides of the laser, is reduced, through lateral confinement of the carriers (Ref 44:207-208).

Although stripe geometry is generally recommended for

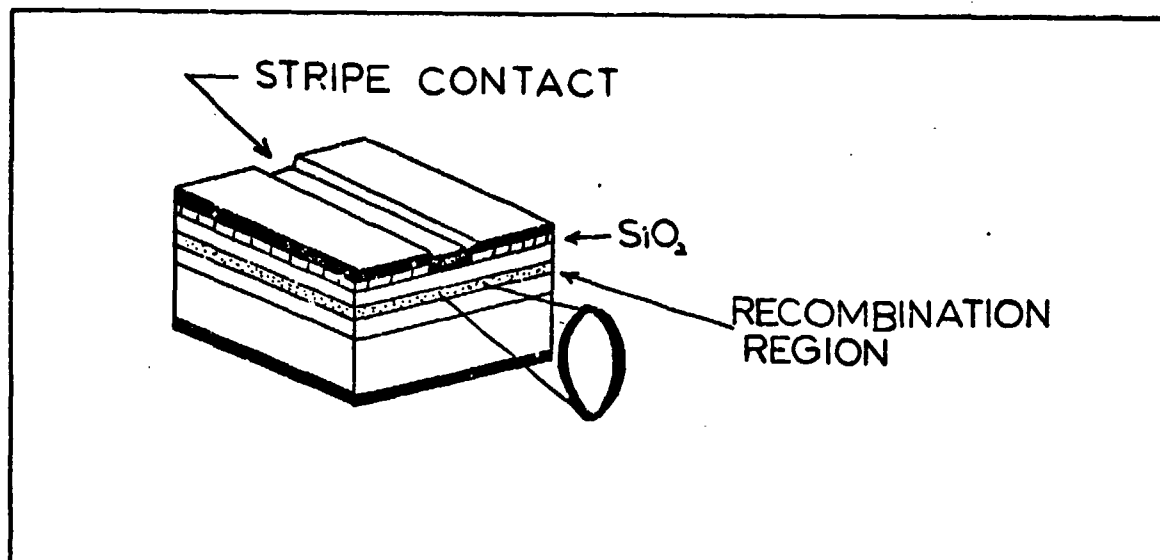


Fig. 17. Typical oxide insulated Stripe Geometry Heterostructure Laser (Ref 39:25)

low-power CW operation of GaAs lasers used in optical communications (Ref 42:94), there is a major disadvantage of this design for the high-power case. With the laser mounted on the heat sink, p side down (Fig. 18), to minimize the junction to heat-sink distance, the SiO_2 acts as a thermal barrier to heat flowing out of the junction into the heat sink (Ref 45:409). The flow of heat is then confined to the dimensions of the stripe as shown in Fig. 18. Consequently, greater power can be obtained from a GaAs laser through the use of broad area contacts or very wide stripe contacts (Ref 45:409).

Summary

The most significant finding in this section is that the maximum output power can be obtained from long lasers (1.5 mm to 2.0 mm) with low end reflectivities (0.010 to

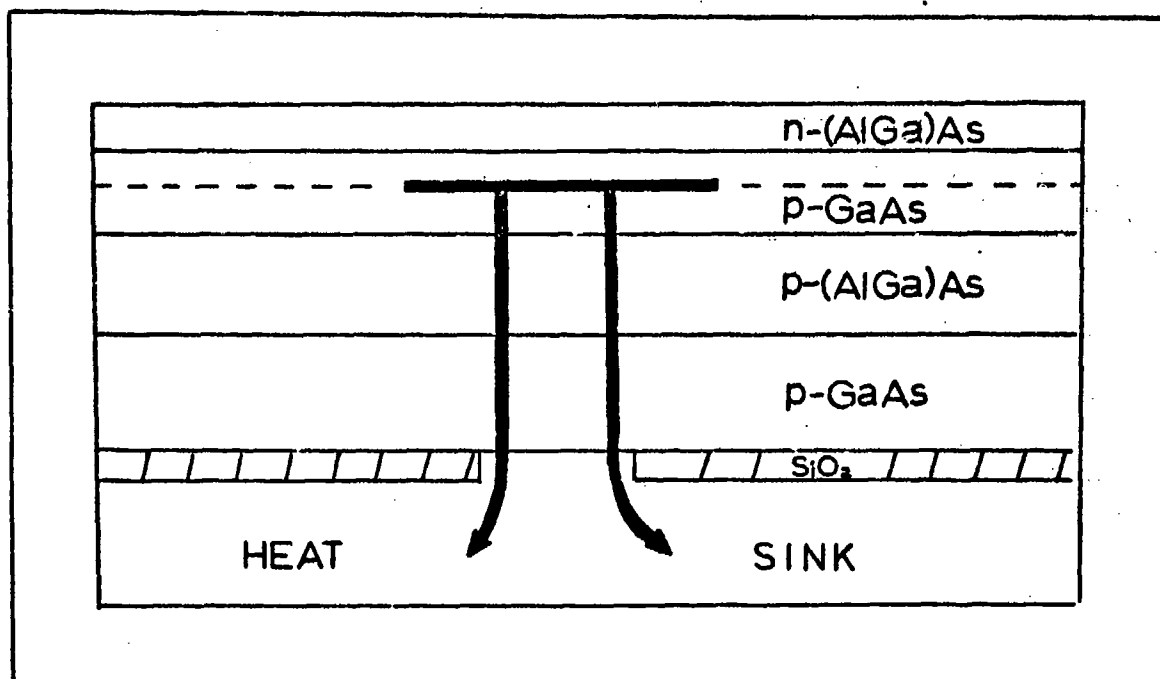


Fig. 18. Thermal Heat Flow Model for oxide insulated stripe geometry heterostructure laser proposed by Garell-Jones (Ref 45:409)

0.002). The maximum output power will be obtained from devices with a small d , but the minimum value of d is ultimately limited by the catastrophic damage limit of the output facet. Wide lasers will also produce more power than narrow ones, but W is limited both by the practical consideration that L must be greater than W , and the thermal restraints on W to be addressed in the next chapter.

Finally, the LOC design is the most suitable design for implementing these results, since the carriers can be confined to a thin recombination region within a thick optical cavity with a large area output facet, that can accommodate the high optical flux present in a high power device.

V. Thermal Effects

The maximum power, which can be obtained from a semiconductor injection laser, operated CW, is ultimately limited by heating in the junction region. Very high temperatures in the junction will contribute to the gradual degradation of the device, discussed in the Appendix, and will eventually alter the normal electronic processes taking place in the crystal, rendering the device unuseable (Ref 46:303). The four major sources of junction heating in the injection laser are: (1) that created by absorption of coherent light, (2) that created by non-radiative recombination of injected carriers, (3) that created by the losses necessary to achieve threshold, and (4) that due to ohmic heating (Ref 47:534).

The most widely used method of lowering the junction operating temperature is by connecting the laser to a heat sink. In 1965 Ciftan and Debye obtained CW power greater than 7.2 W from a homojunction GaAs laser, operated at 4.2K, through contact with a liquid Helium cooled heat sink (Ref 48). Other early experiments concentrated on optimizing laser performance utilizing a double-sided heat sink cooled to liquid nitrogen temperature of 77K (Refs 49; 50; 51). A typical example of the double-sided heat sink is shown in Fig. 19. Copper is the most popular choice for a

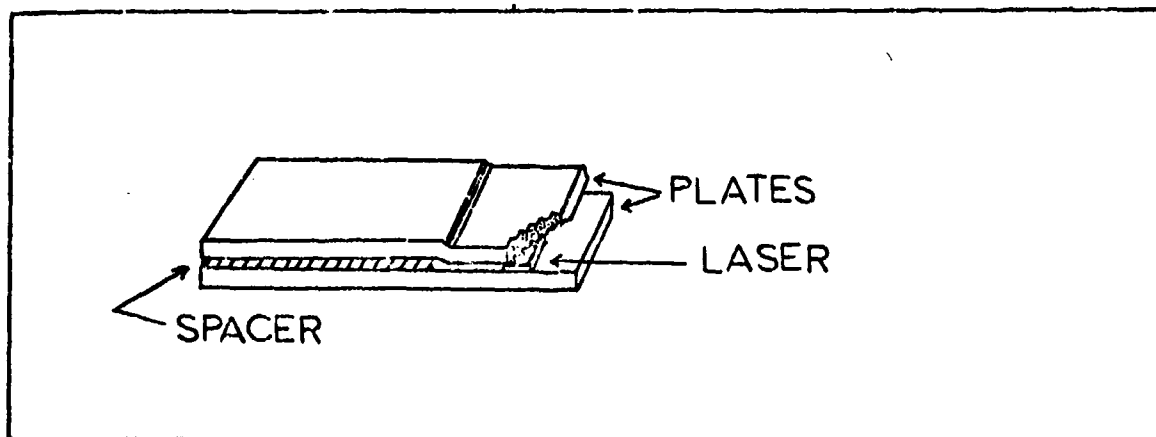


Fig. 19. Double-Sided heat sink proposed by Marinace
(Ref 49:543)

heat-sink material, due to its very high thermal conductivity and relatively low cost (compared to gold, for example). Copper and GaAs, however, have significantly different thermal expansion coefficients (Ref 42:94). This is believed to be the cause of crystal "microcracks" observed in the GaAs when the laser is operated in a double-sided heat sink, through several thermal cycles from 77K to room temperature (Ref 52:30). As a result, most of the recent lasers, designed for cryogenic operation utilize single-sided heat sinks (Ref 6:27; 45:409). For optimum removal of heat from the junction, using a single-sided heat sink, the junction to heat-sink distance must be as small as possible.

Studies of the optimum laser length and width resulting in maximum CW power output, based on thermal limitations have been accomplished by Vilms et al. (Ref 53) and Pilkuhn and Guettler (Ref 54) for homostructure lasers.

The analysis by Pilkuhn and Guettler is more recent (1968) and comprehensive. In their analysis they assumed the rectangular Fabry-Perot cavity could be approximated by an ellipse, in order to calculate the thermal spreading resistance, Z_{th} (Ref 46:308). For their model, they obtained the following expression for P_{stim} , the laser output due to stimulated emission (Ref 54:134):

$$P_{stim} = V\eta_{ext} \left\{ \frac{1}{2R_s} \left[\left(v^2(1 - \eta_{ext})^2 + \frac{4\Delta TR_s}{Z_{th}} - 4VI_t R_s \eta_{ext} \right)^{1/2} - V(1 - \eta_{ext}) \right] - I_t \right\} \quad (30)$$

where R_s is the series resistance and

$$R_s = \frac{\rho d}{LW} \quad (31)$$

and Z_{th} is the spreading resistance and

$$Z_{th} = \frac{K(1 - W^2/L^2)}{2\sqrt{\pi}\kappa L} \quad (32)$$

where $K(k) = F(k, \pi/2)$ is a complete elliptic integral of the first kind (Ref 55:767-768), κ is the thermal conductivity, W is the laser width, L is the laser length, I_t is the threshold current, V is the voltage such that eV is the bandgap energy, and η_{ext} is the external quantum efficiency with

$$\eta_{ext} = \frac{\eta_i}{1 + \frac{\alpha L}{\ln(1/R)}} \quad (27)$$

where η_i is the internal quantum efficiency, α the total internal absorption coefficient, and R is the reflectivity. Pilkuhn and Guettler determined that for constant R of 0.215 that the optimum values of L and W to maximize P_{stim} were 4.5×10^{-2} cm and 1×10^{-3} cm respectively (Ref 54: 134-135). P_{stim} , however, may be further increased, by changing R (this was not done by Pilkuhn and Guettler).

Appropriate substitution of Eqs (31) and (32) into Eq (30) yields the following expression for P_{stim} :

$$P_{stim} = (LW)V\eta_{ext} \left\{ \left[\left(\frac{V(1 - \eta_{ext})}{2\rho d} \right)^2 + \frac{2\sqrt{\pi}\kappa\Delta T}{dWK(1 - W^2/L^2)} - \frac{VJ_t\eta_{ext}}{\rho d} \right]^{1/2} - \frac{V(1 - \eta_{ext})}{2\rho d} - J_t \right\} \quad (33)$$

where J_t is the threshold current density. In addition to the term LW , which has been factored out of Eq (33), L and W are found in the η_{ext} terms and in the term $2\sqrt{\pi}\kappa\Delta T / \rho dWK(1 - W^2/L^2)$. Assuming a constant absorption coefficient, if L is varied, R can be changed an appropriate amount such that a constant external quantum efficiency can be maintained as was done in Chapter IV. For example, let $\eta_i = 1$, $\alpha = 6\text{cm}^{-1}$, $L = 350$ micrometers and $R = 0.3$, then from Eq (27), $\eta_{ext} = 0.85$ and from Eq (28) C is equal to 34.4 cm^{-1} . If C is held constant, and L is doubled to equal 700 micrometers, then solution of the expression

$$R = e^{-CL} \quad (34)$$

will yield a reflectivity of 0.09, which when used with the new length of 700 micrometers in Eq (27) will yield the original external quantum efficiency of 0.85. Using this assumption, then, that for any value L , a constant external quantum efficiency can be maintained. Similarly, the value of J_t , which also contains the parameter C (Ref Eq [22]) can also be maintained at a constant value for any value of L by appropriately changing the reflectivity.

Next, the term $2\sqrt{\pi}K\Delta T / \rho dWK(1 - W^2/L^2)$ will be considered. The elliptic integral $K(1 - W^2/L^2)$ will reach a minimum when $W = L$. Therefore, taking into account the W in the denominator, the entire term will reach a maximum (contributing the most to P_{stim}) for a very small W equal to a very small L . However, the dominant term in Eq (33) is the LW factor out front, indicating P_{stim} will increase with increasing L and W .

P_{stim} is plotted as a function of L , for W equal to 50, 100, 150, and 200 micrometers in Fig. 20, using the following assumptions: $T_{heat\ sink} = 77K$; $\eta_i = 1$ (Ref 54); α is approximately constant at 6 cm^{-1} over a limited range of L ; $V = 1.5\text{ Volts}$ (Ref 54:134); and finally, R is altered an appropriate amount for each value of L to maintain a constant η_{ext} of 0.83 and a constant J_t of 500 A/cm^2 as discussed above.

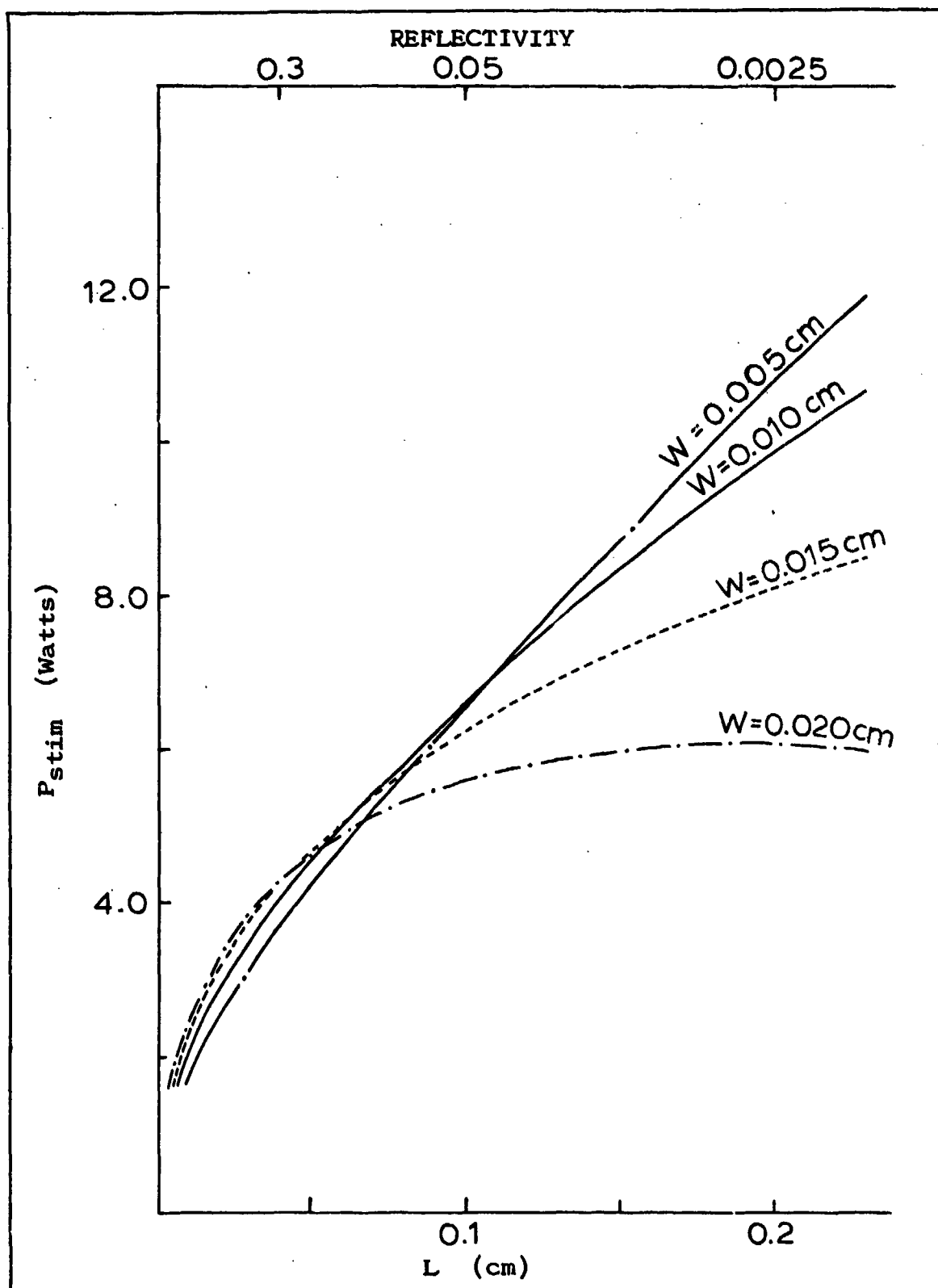


Fig. 20. Stimulated Power vs Laser Length for Different Values of Width ($J_t = 500 \text{ A/cm}^2$; $C = 30.0 \text{ cm}^{-1}$; $V = 1.5 \text{ Volts}$; $\kappa = 2 \text{ W/cm deg}$; $T = 10\text{K}$; $\rho_d = 1 \times 10^{-6} \Omega \text{ cm}^2$; $\eta_{ext} = 0.83$)

The resultant plot of Fig. 20 indicates that for short lasers, the output power increases with increasing length and width, as was determined in Chapter IV (Ref: Fig. 13). However, for long lasers (L greater than 0.5 mm), the trend of output power as a function of laser width W , is different. The results of this chapter indicate that maximum power can be obtained from a narrow (small W) laser. There is a tradeoff between these results in a device with realistic dimensions. Based on the reported performance of existing devices, a laser width of 50 to 100 micrometers would be a reasonable parameter. A device with length L , greater than 1 mm, then could theoretically yield a CW output power of several watts.

VI. Conclusions and Recommendations

It is strikingly clear from the results of Chapters IV and V, that the output power of a semiconductor laser can be dramatically increased by increasing the laser length, L . The magnitude of the width, W , is limited by the thermal considerations, discussed in Chapter V. From Fig. 20, it can be seen that the greatest power per unit length can be achieved from devices with a relatively small W (near 50 micrometers). The output power can be further optimized by choosing an appropriate value of reflectivity, R , for the selected L , that will result in the maximum external quantum efficiency from Eq (27). Altering the reflectivity can be readily accomplished by coating the output facet of the laser with a dielectric antireflective film.

These results are precisely those that would be expected in light of basic laser theory and the behavior of solid state and gas dynamic lasers. If the volume of the active region is increased, by increasing the length of the lasing medium, then there will be more injected electrons involved in the process of stimulated emission, resulting in the production of more photons, and hence greater total output power.

A principal difference between semiconductor lasers

and other lasers, however, is that the thickness, t , of the active region, must be maintained at a small value (between 0.25 to 1.00 micrometers) compared to the diffusion length of the minority carriers, so that uniform excitation of the active region can be achieved. Theoretically, if the thickness, d , of the optical cavity is decreased, so that it is equal to the value of t (in which case the device becomes a DH laser) the maximum output power will be realized. Realistically, however, there is a limit to the magnitude of the optical flux density, that can be tolerated by the output facet (Ref Appendix). The LOC laser proposed by Lockwood et al. has the unique feature, that the active region thickness, t , can be maintained small, while increasing the optical cavity thickness, d , through proper variation of the Aluminum content in the layers of the heterostructure. A larger d will result in a larger output facet area, capable of withstanding a greater total optical flux, compared to the generally small facet area common to DH lasers.

The goal of this thesis has been to study the parameters which will affect the maximum power yield of a single device. Obviously even greater total power may be achieved by connecting several devices together in an amplifier chain. This technique has already been successfully implemented in a variety of systems for the Air Force (Refs 56; 57) and Army (Ref 58).

In light of the results of this thesis, the following recommendations are presented for the continuation of the

solution to the overall high power CW problem. A study of new crystal growth procedures and methods such as MOCVD, would reveal which process would be most suitable for the fabrication of long (greater than 1 mm) lasers. Improvements in heat-sink design, particularly in the method the laser is bonded to the heat sink are needed to achieve the most efficient evacuation of heat from the device.

Although the material parameters of GaAs and $\text{Al}_x\text{Ga}_{1-x}\text{As}$ were used in the output power computations of Chapters IV and V, further study would be appropriate to determine if lasers fabricated from other semiconductor materials could produce even greater power. From Eq (30), it can be seen that material parameters such as absorption, bandgap energy, and electrical and thermal conductivity will affect the CW output power of a semiconductor laser.

In conclusion, then, a long narrow heterostructure laser with a thin optical cavity (W of the order of 50 to 100 micrometers and L greater than 1 mm) having a low end reflectivity, shows the best promise of yielding the maximum CW output power.

Bibliography

1. Triodle, B. J. KA-98/RPV Demonstration Test Program Final Report #12761. Norwalk, Conn.: Perkin-Elmer Corporation, Electro-Optical Division, 5 December 1975.
2. Paulson, R. F., Air Force Avionics Laboratory (Private Communication). Wright Patterson AFB, Ohio, September 19, 1978.
3. Copeland, John A. "CW Operation of LSA Oscillator Diodes--44 to 88 GHz," The Bell System Technical Journal, 46: 284-287 (January 1967).
4. Boisrobert, C. Y., Debeau, J., and Hartog, A. H. "Sinusoidal Modulation of a CW GaAs Laser from 9 MHz to 1.1 GHz," Optics Communications, 19: 305-307 (November 1976).
5. Arnold, G. and Russer, P. "Modulation Behavior of Semiconductor Injection Lasers," Applied Physics, 14: 255-268 (November 1977).
6. Gill, R. B. and Stockton, T. E. CW GaAs Diode Laser. AFAL-TR-76-173. Wright-Patterson AFB, Ohio: Air Force Avionics Laboratory, May 1977. (AD-B020483).
7. Murawinski, Daniel J. Characterization of High Power GaAs Lasers. Unpublished thesis. Wright-Patterson Air Force Base, Ohio: Air Force Institute of Technology, December 1977. (GEP/PH/77-9).
8. Yariv, Amnon. Introduction to Optical Electronics. (Second edition). New York: Holt Rheinhardt and Winston, 1976.
9. Kittel, C. Elementary Statistical Physics. New York: John Wiley and Sons, Inc., 1958.
10. Einstein, A. "Zur Quantentheorie der Strahlung," Physikalische Zeitschrift, 18: 121-128 (March 1917) (In German).
11. SZE, S.M. Physics of Semiconductor Devices. New York: John Wiley and Sons, Inc., 1969.
12. Rieck, Heinrich. Semiconductor Lasers. London: Macdonald & Co. Ltd., 1970.

13. Leyngel, Bela A. Lasers (Second edition). New York: John Wiley and Sons, Inc., 1971.
14. Stern, F. "Semiconductor Lasers: Theory," Laser Handbook, Volume I. New York: North Holland Publishing Company, 1972.
15. Nathan, M. I., Dumke, W. P., Burns, G., Dill, F. H., and Lasher, G. J. "Stimulated Emission of Radiation from GaAs p-n Junctions," Applied Physics Letters, 1: 62-64 (November 1962).
16. Quist, T. M., Rediker, R. H., Keyes, R. J., Krag, W. E., Lax, B., McWhorter, A. L., and Zeiger, H. J. "Semiconductor Maser of GaAs," Applied Physics Letters, 1: 91-92 (December 1962).
17. Hall, R. N., Fenner, G. E., Kingsley, J. D., Soltys, T. J., and Carlson, R. O. "Coherent Light Emission from GaAs Junctions," Physics Review Letters, 9: 366-368 (November 1962).
18. Holonyak, N. and Bevacqua, S. F. "Coherent (Visible) Light Emission from Ga(As_{1-x}P_x) Junctions," Applied Physics Letters, 1: 82-83 (December 1962).
19. Panish, Morton B. "Heterostructure Injection Lasers," Proceedings of the IEEE, 64: 1512-1540 (October 1976).
20. Kroemer, H. "A Proposed Class of Heterojunction Injection Lasers," Proceedings of the IEEE, 51: 1782-1783 (December 1963).
21. Kressel, H. "Semiconductor Lasers: Devices," Laser Handbook Volume I. New York: North Holland Publishing Company, 1972.
22. Lockwood, H. F., Kressel, H., Sommers, H. S., Jr., and Hawrylo, F. Z. "An Efficient Large Optical Cavity Injection Laser," Applied Physics Letters, 17: 499-502 (December 1970).
23. Cho, A. Y., Dixon, R. W., Casey, H. C., and Hartman, R. L. "Continuous Operation of GaAs-Al_xGa_{1-x}As DH Lasers Prepared by Molecular Beam Epitaxy," Applied Physics Letters, 28: 501-503 (May 1976).
24. Dupis, R. D. and Dapkus, P. D. "Room-Temperature Operation of Ga_{1-x}Al_xAs/GaAs Double-Heterostructure Lasers Grown by Metalorganic Chemical Vapor Deposition," Applied Physics Letters, 31: 466-468 (October 1977).

25. Kogelnik, H. and Shank, C. V. "Stimulated Emission in a Periodic Structure," Applied Physics Letters, 18: 152-154 (February 1971).
26. Namizaki, Shams, M. K., and Wang, S. "Large-Optical-Cavity GaAs-(GaAl)As Injection Laser with Low-Loss Distributed Bragg Reflectors," Applied Physics Letters, 31: 122-124 (July 1977).
27. Matsumoto, N. and Kumabe, K. "AlGaAs-GaAs Semiconductor Ring Laser," Japanese Journal of Applied Physics, 16: 1395-1398 (August 1977).
28. Afromowitz, Martin A. "Thermal Conductivity of $Ga_{1-x}Al_xAs$ Alloys," Journal of Applied Physics, 44: 1292-1294 (March 1973).
29. Baird, J. R., Carr, W. N., and Reed, B. S. "Analysis of a GaAs Laser," Transactions of the Metallurgical Society of the AIME, 230: 286-290 (March 1964).
30. Ulbrich, R. and Pilkuhn, M. H. "Influence of Reflectivity on the External Quantum Efficiency of GaAs Injection Lasers," IEEE Journal of Quantum Electronics, QE-6: 314-316 (June 1970).
31. Ettenberg, M., Lockwood, H. F., and Sommers, H. S. "Radiation Trapping in Laser Diodes," Journal of Applied Physics, 43: 5047-5051 (December 1972).
32. Nannichi, Y. "Recent Progress in Semiconductor Lasers," Japanese Journal of Applied Physics, 16: 2089-2102 (December 1977).
33. Casey, H. C., Jr. and Panish, M. B. Heterostructure Lasers (Part A: Fundamental Principles). New York: Academic Press, 1978.
34. Cheroff, G., Stern, F., and Triebwasser, S. "Quantum Efficiency of GaAs Injection Lasers," Applied Physics Letters, 2: 173-174 (May 1963).
35. Adams, M. J. and Cross, M. "Electromagnetic Theory of Heterostructure Lasers," Solid State Electronics, 14: 865-883 (September 1971).
36. Goodwin, A. R. and Selway, P. R. "Gain and Loss Processes in GaAlAs-GaAs Heterostructure Lasers," IEEE Journal of Quantum Electronics, QE-6: 285-290 (June 1970).

37. Kressel, H., Lockwood, H. F., and Hawrylo, F. Z. "Large-Optical-Cavity (AlGa)As-GaAs Heterojunction Laser Diode: Threshold and Efficiency," Journal of Applied Physics, 43: 561-567 (February 1972).
38. Hwang, C. J., Patel, N. B., Sacilotti, M. A., Prince, F. C., and Bull, D. J. "Threshold Behavior of (GaAl)As-GaAs Lasers at Low Temperatures," Journal of Applied Physics, 49: 29-34 (January 1978).
39. Kressel, H., Lockwood, H., Ettenberg, M., and Ladany, I. "Light Sources for Fiber Optic Communications," RCA Engineer, 22: 22-28 (December 1976).
40. Bourne, W. O., Goodwin, A. R., Pion, M., and Selway, P. R. "Dauerstrich-Laser fur die Optische Nachrichtenubertragung (Continuous-Wave Laser for Optical Communication)," Nachrichten Elektronik, 31: 7-10 (January 1977) (In German).
41. Lindstrom, C. and Janson, M. "13 Micron Wide Stripe CW GaAs/GaAlAs DH Lasers Linear to More Than 10mW," Electronics Letters, 14: 172-174 (March 1978).
42. Selway, P. R. "Recent Developments in Semiconductor Injection Lasers," Electronic Engineering, 49: 93-96 (June 1977).
43. Ettenberg, M., Hudson, K. C., and Lockwood, H. F. "High-Radiance Light Emitting Diodes," IEEE Journal of Quantum Electronics, QE-9: 987-991 (October 1973).
44. Casey, H. C., Jr. and Panish, M. B. Heterostructure Lasers (Part B: Materials and Operating Characteristics). New York: Academic Press, 1978.
45. Garell-Jones, P. and Dymont, J. C. "Calculations of the Continuous-Wave Lasing Range and Light-Output Power for Double-Heterostructure Lasers," IEEE Journal of Quantum Electronics, QE-11: 408-413 (July 1975).
46. Keyes, R. W. "Thermal Problems of the Injection Laser," IBM Journal of Research and Development, 9: 303-314 (July 1965).
47. Lasher, G. J. and Smith, W. V. "Thermal Limitations on the Energy of a Single Injection Laser Light Pulse," IBM Journal of Research and Development, 8: 532-536 (November 1964).
48. Ciftan, M. and Debye, P. P. "On the Parameters Which Affect the C. W. Output of GaAs Lasers," Applied Physics Letters, 6: 120-121 (March 1965).

49. Marinace, J. C. "High Power CW Operation of GaAs Injection Lasers at 77°K," IBM Journal of Research and Development, 7: 543-544 (November 1964).
50. Engeler, W. E. and Garfinkel, M. "Characteristics of a Continuous High-Power GaAs Junction Laser," Journal of Applied Physics, 35: 1734-1741 (June 1964).
51. Dierschke, E. G. CW Ga As Diode Laser. AFAL-Tr-75-123. Wright-Patterson AFB, Ohio: Air Force Avionics Laboratory, May 1977.
52. Kressel, H. and Byer, N. E. "Physical Basis of Non-catastrophic Degradation in GaAs Injection Lasers," Proceedings of the IEEE, 57: 25-33 (January 1969).
53. Vilms, J., Wandinger, L., and Klohn, K. L. "Optimization of the Gallium Arsenide Injection Laser for Maximum C. W. Power Output," IEEE Journal of Quantum Electronics, QE-2: 80-83 (April 1966).
54. Pilkuhn, M. H. and Guettler, C. T. "Optimum Stimulated Light Powers from GaAs Injection Lasers," IEEE Journal of Quantum Electronics, QE-4: 132-135 (April 1968).
55. Weast, Robert C. and Selby, Samuel M. Chemical Rubber Company Handbook of Tables for Mathematics (Third edition). Cleveland, Ohio: The Chemical Rubber Company, 1967.
56. Barratt, W. and O'Hara, L. High Radiance AlGaAs Illuminator. AFAL-TR-74-208. Wright-Patterson AFB, Ohio: Air Force Avionics Laboratory, November 1974. (AD-A007976).
57. Fulton, J. T. and Kaplan, I. High Average Power Diode Laser Illuminator. AFAL-TR-74-162. Wright-Patterson AFB, Ohio: Air Force Avionics Laboratory, May 1975. (AD-A011692).
58. Nuese, J., Olsen, G. H., Ettenberg, M., and Enstrom, R. E. High Power 1.06 micrometer Injection Lasers. ECOM-75-0856-F. Fort Monmouth, New Jersey: US Army Electronics Command, July 1976. (AD-B013377).
59. Kressel, H. and Mierop, H. "Catastrophic Degradation in GaAs Injection Lasers," Journal of Applied Physics, 38: 5419-5421 (September 1967).
60. Kressel, H. and Ladany, I. "Reliability Aspects and Facet Damages in High-Power Emission from (AlGa)As CW Laser Diodes at Room Temperature," RCA Review, 30: 230-239 (June 1975).

61. Kressel, H., Ettenberg, M., and Ladany, I. "Accelerated Step-Temperature Aging of $\text{Al}_x\text{Ga}_{1-x}\text{As}$ Heterojunction Laser Diodes," Applied Physics Letters, 32: 305-308 (March 1978).
62. Chinone, N., Nakashima, H., and Ito, R. "Long-Term Degradation of $\text{GaAs-Ga}_{1-x}\text{Al}_x\text{As}$ DH Lasers Due to Facet Erosion," Journal of Applied Physics, 48: 1160-1162 (March 1977).
63. Ettenberg, M., Sommers, H. S., Jr., Kressel, H., and Lockwood, H. F. "Control of Facet Damage in GaAs Diodes," Applied Physics Letters, 18: 571-573 (June 1971).
64. Ladany, I., Ettenberg, M., Lockwood, H. F., and Kressel, H. " Al_2O_3 Half-Wave Films for Long-Life CW Lasers," Applied Physics Letters, 30: 87-88 (January 1977).

Appendix

Laser Degradation

Degradation Phenomena

Several previous studies of GaAs lasers indicate that two types of degradation occur in these devices. Lasers operated at very high power suffer from "catastrophic degradation"; and, "gradual degradation" of lasers operated CW at high power levels has been observed.

Catastrophic degradation of GaAs lasers is characterized by the formation of pits or grooves in the laser facets followed by complete laser failure. This phenomenon is believed to be directly related to the optical flux density at the output facet (Ref 59:5419). An unexpected but most significant result of experiments by Kressel and Mierop with pulsed homojunction lasers indicate that catastrophic degradation will occur at a lower output power for devices operating at 77K than for devices operating at 300K. The facet damage is believed to be caused by stimulated Brillouin emission and the consequent formation of destructive acoustical waves (Ref 59:5419). The temperature dependence is assumed to occur because of the increase of the acoustic phonon mean free path with decreasing temperature (Ref 59:5420). The damage mechanism was observed by Kressel and Mierop to occur at 1.8 to 2.5 MW/cm² at 77K and 5.8 to 8 MW/cm² at 300K for pulsed lasers (Ref 59:5420).

The damage threshold for lasers operated CW is considerably lower. An experimental study of "stripe geometry" heterostructure lasers operated CW was conducted by Ladany and Kressel (Ref 60). Failure of the devices occurred at 23 to 35 mW output in the diodes with 13 micrometer stripes and 90 to 100 mW output in the diodes with 50 micrometer wide stripes (Ref 60:233). These results indicate an optical flux of approximately 0.20 to 0.42 MW/cm² at failure, which is an order of magnitude lower than the damage threshold for pulsed lasers. In addition it was noted that the threshold for damage was even lower than these figures if dust or other foreign materials were present on the surface of the facet (Ref 60:236). Finally, it has been observed that lasers which originally had an irregular near field mode pattern (as a result of inherent crystal imperfections) degraded much more rapidly than those with a uniform mode pattern (Ref 52:29).

Non-catastrophic or gradual degradation is a more complex phenomenon. Research conducted by Kressel and Byer (Ref 52) indicates that the dominant factor in this process is a gradual reduction in the internal radiative quantum efficiency. After a long operating time, "beady" laser emission becomes noticeable (Ref 52:28). These beads grow, creating a phenomenon that has come to be known as Dark Line Defects (DLD). Further research by Kressel et al. with GaAlAs lasers (Ref 61:305-306) suggests that the cause of this degradation is the formation of non-radiative

impurity centers through non-radiative electron hole recombination. Two significant results of this research are: (1) gradual degradation of the laser occurs much faster at high temperature; and, (2) gradual degradation of CW lasers occurs more rapidly than degradation of pulsed lasers (Ref 61:307).

Lasers operated CW over long periods of time exhibit "facet erosion," which is different from catastrophic "facet damage," discussed previously. Results obtained by Chinone et al. indicate that this facet erosion and consequent decrease in output efficiency is directly proportional to the optical flux density (Ref 62:1160-1161).

Control of Laser Degradation

Operation of GaAs lasers at high CW power output, then, results in both gradual and catastrophic degradation.

Catastrophic degradation due to laser facet damage can be controlled to some extent through the use of oxide coatings on the laser facet. Experiments conducted by Ettenberg et al. (Ref 63) have shown that a coating of SiO₂ to reduce the facet reflectivity has proven effective in increasing the threshold for catastrophic damage. Experiments conducted by Ladany et al. (Ref 64) indicate that gradual facet erosion can be controlled by coatings of Al₂O₃.

Some combination of these techniques would be beneficial for increasing the lifetime and damage threshold of

the RF modulated, DC biased diode (the device of primary concern for this thesis), which is subject to both the catastrophic degradation normally associated with pulsed lasers and the gradual degradation normally associated with CW lasers. Gradual degradation due to the formation of non-radiative impurity centers is a phenomenon that is not well understood. Further research in this area is warranted. The damage mechanism for catastrophic degradation is directly related to the optical flux through the facet. Increasing the dimensions of the laser facet would permit tolerance of a greater total power by the output facet. Finally, imperfections in the crystal, resulting from crystal growth and preparation, have a serious effect on the optimum power which can be sustained in a GaAs laser. Technological advances in the preparation of these crystals such as LPE, VPE, MBE, and MOCVD may make it possible to develop purer crystals than have been used previously.

Vita

Captain John C. Griffin, III was born on 30 March 1947 in Brooklyn, New York, the son of John C. Griffin, Jr. and Sally A. Griffin. After graduating from Brooklyn Preparatory School in 1964, he attended St. Joseph's College in Philadelphia, Pennsylvania. He graduated from St. Joseph's in June 1968 with a Bachelor of Science degree in Physics and received his commission as a second lieutenant through the AFROTC program. After completing the USAF Undergraduate Navigator Training program at Mather AFB, California and upgrade training as an RF-4C Weapon Systems Officer at Shaw AFB, South Carolina in 1970, he served a combat tour in the RF-4C at Tan Son Nhut AB, Vietnam. In November 1971, Captain Griffin returned to Shaw AFB as an Instructor Weapon Systems Officer in the 33rd Tactical Reconnaissance Training Squadron. He then served as an Instructor Weapon Systems Officer and Radar Systems Officer while assigned to the 26th Tactical Reconnaissance Wing at Zweibruecken Air Base, Germany from April 1973 to May 1976. He completed the Engineering Sciences program at the School of Engineering, Air Force Institute of Technology prior to entering the master's degree program in Electro-Optics at AFIT in June 1977. Captain Griffin is married to the former Janet Y. Witbeck of El Monte, California and has one son, John.

Permanent Address: 7410 Louisa Allen Court

San Antonio, Texas 78240